

Cross-Audit Projection for Model Risk Prediction

YIJIAN HUANG

Department of Biostatistics and Bioinformatics, Emory University,

Atlanta, Georgia 30322, U.S.A.

yhuang5@emory.edu

ABSTRACT

For training-data-based model risk prediction, K -fold cross-validation (CV) is widely used to mitigate the well-known over-optimism of the empirical risk and is often regarded as reliable. However, for binary classification via empirical risk minimization, our numerical studies reveal a surprising phenomenon: K -fold CV may perform poorly in estimating class-specific risks, even worse than the empirical estimator. We perform a higher-order asymptotic analysis showing that K -fold CV may converge at a slower rate, whereas the empirical estimator exhibits a second-order asymptotic bias that explains its over-optimism. These findings motivate a novel two-step procedure for model risk prediction, termed cross-audit projection (CAP). The cross-audit step adopts the same resampling scheme as K -fold CV to estimate over-optimism in subsamples, while the asymptotic-theory-informed projection step adjusts for the reduced sample size in bias correction of the empirical risk. The resulting CAP estimator is first-order asymptotically equivalent to the empirical risk while achieving second-order asymptotic unbiasedness. An accompanying inference procedure is also developed. Simulation studies support theoretical advantages of CAP and demonstrate favorable finite-sample performance. An application to breast cancer detection further illustrates the proposed method.

KEY WORDS: Asymptotic bias; Bias correction; Binary classification; Cross-validation; Empirical risk minimization; Over-optimism.

1. INTRODUCTION

Once a predictive model is trained, its performance in future applications needs to be evaluated to inform potential deployment. The empirical risk is well known to be optimistically biased. Although independent validation is conceptually natural, reserving data for this purpose leads to inefficient use of typically limited samples. Accurate model risk prediction based on the training data has long been pursued.

Classical approaches seek to correct empirical risk analytically, as in Mallows' C_p (Mallows, 1973), AIC (Akaike, 1974), and covariance penalties (Stein, 1981; Efron, 2004). However, these methods are model-based, restrictive in their choice of loss function, and are not well suited to increasingly complex modern predictive algorithms. Resampling-based methods provide a natural alternative to overcome these limitations. Harrell, Lee, and Mark (1996) corrected empirical risk using the nonparametric bootstrap for bias estimation. Nevertheless, the bias may not be eliminated because bootstrap resamples overlap with the original data. Cross-validation (CV) methods (Allen, 1974; Geisser, 1975; Stone, 1974, 1977), which keeps training and validation subsamples mutually exclusive, have become the predominant tools. Depending on how training subsamples are constructed, variants include leave-one-out CV, K -fold CV with a typical choice of $K = 10$, repeated K -fold CV, repeated learning-testing schemes (Burman, 1989), and bootstrap-based methods such as the 0.632 and 0.632+ rules (Efron, 1983; Efron and Tibshirani, 1997).

Among CV methods, K -fold CV is perhaps the most widely used owing to its conceptual simplicity and moderate computational cost; in contrast, leave-one-out CV can be computationally prohibitive for modern learning algorithms. However, we reveal a previously undocumented phenomenon that K -fold CV may perform poorly despite its perceived reliability, through an example of binary classification via empirical risk minimization (ERM).

EXAMPLE 1. (ERM CLASSIFIER WITH A SINGLE FEATURE) This binary classification

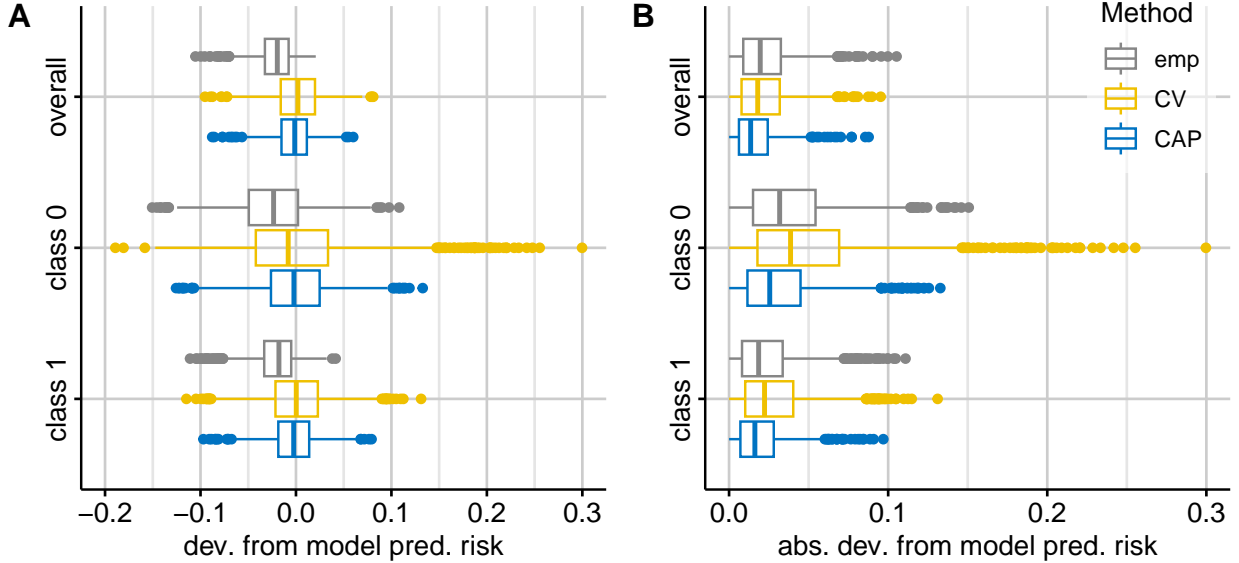


Figure 1: Simulation results on empirical, 10-fold CV, and proposed CAP estimators of overall and class-specific model prediction risks in single-feature binary ERM classification with $X_0 \sim N(0, 1)$, $X_1 \sim N(1, 1)$, $\omega = 0.25$, and $n_0 = n_1 = 100$, based on 1000 simulated datasets. Panel A: Boxplots of deviations from model prediction risks. Panel B: Boxplots of absolute deviations from model prediction risks.

is based on the dichotomization of a single feature, denoted by X_d for class $d \in \{0, 1\}$. To accommodate differential costs of class-specific misclassification, the overall risk is defined as a weighted sum of class-specific misclassification rates, with weights ω and $1 - \omega$ for classes 0 and 1, respectively. A classifier that minimizes the overall risk is considered optimal, and ERM is employed for the estimation. Suppose that n_d independent replicates of X_d are observed for each class $d = 0, 1$. Figure 1 presents simulation results of the empirical risks and 10-fold CV estimates. As expected, CV mitigated over-optimism of the empirical risks, overall and class-specific alike. However, surprisingly CV tracked the class-specific risks even less accurately than the empirical estimator.

Through internal validation, K -fold CV directly and unbiasedly targets the average risk of the K subsample models, known as the *CV ensemble prediction risk*. Its discrepancy from the model prediction risk is commonly assumed to be negligible. The same premise also underlies several inferential procedures. Dudoit and van der Laan (2005), Austern

and Zhou (2020), and Bayle et al. (2020) established central limit theorems for K -fold CV with respect to the CV ensemble prediction risk for various learning algorithms, and the resulting methods have been used to draw inference on the model prediction risk; see also LeDell, Petersen and van der Laan (2015) and Benkeser, Petersen and van der Laan (2020). Bates, Hastie and Tibshirani (2024) proposed an additional inference procedure based on K -fold CV. However, in light of the unexpected phenomenon observed in Example 1, a closer examination of K -fold CV is warranted, along with a broader question of whether alternative methods can improve the estimation and inference of model prediction risk. To address these issues, we will consider general linear ERM classification and conduct an asymptotic study to elucidate the anomalous behavior of K -fold CV, as well as the over-optimism of empirical risk. These findings motivate a novel method termed cross-audit projection (CAP). For a preview, Figure 1 also presents the CAP estimates, illustrating their superior performance.

The contributions of this article are four-fold. First, to our knowledge, we demonstrate for the first time that K -fold CV may perform worse than the empirical risk. Second, we establish a higher-order asymptotic analysis framework to characterize both bias and variability in model risk prediction. This framework clarifies the over-optimism in the empirical risk through second-order asymptotic bias and reveals limitations of K -fold CV. Third, and most importantly, we develop the CAP method for accurate model risk prediction by devising an asymptotic-theory-informed resampling procedure. Finally, we provide a refined treatment of ERM for binary classification that is of independent interest. The remainder of the article is organized as follows. Section 2 formulates linear ERM classifier and establishes its asymptotic properties. Section 3 investigates the asymptotic behaviors of empirical and K -fold CV risk estimators, which in turn motivate the CAP procedure for point prediction and inference. Simulation studies and an application to breast cancer detection are presented in Section 4. Section 5 concludes with a discussion. Technical proofs are deferred to the Appendix, with additional results provided in the Supplementary Materials.

2. LINEAR ERM CLASSIFICATION

Consider binary classification with an m -vector feature, \mathbf{X}_d , for $m \geq 1$ and class $d \in \{0, 1\}$. A linear classifier indexed by $(m+1)$ -vector coefficient \mathbf{b} predicts the class label as $I(\mathbf{b}^\top \mathbf{X}_d^\circ > 0)$, where $\mathbf{X}_d^\circ \equiv (\mathbf{X}_d^\top, 1)^\top$; the last component of \mathbf{b} represents minus threshold for the feature combination. The two class-specific risks and overall risk are given by

$$\psi_0(\mathbf{b}) = \Pr(\mathbf{b}^\top \mathbf{X}_0^\circ > 0), \quad \psi_1(\mathbf{b}) = \Pr(\mathbf{b}^\top \mathbf{X}_1^\circ \leq 0), \quad \psi(\mathbf{b}) = \omega\psi_0(\mathbf{b}) + (1 - \omega)\psi_1(\mathbf{b});$$

recall that $\omega \in (0, 1)$ is a user-specified relative weight between the two classes. Two classifiers are said to be *parallel* if their coefficients differ by a scaling factor; such classifiers have identical risks. The optimal classifier minimizes the overall risk, subject to a norm constraint for identifiability:

$$\boldsymbol{\beta} = \arg \min_{\mathbf{b}: \|\mathbf{b}\|_1=1} \psi(\mathbf{b}),$$

where $\|\cdot\|_1$ denotes the ℓ_1 norm. The choice of ℓ_1 norm will facilitate computation in classifier learning but is otherwise non-essential.

2.1 Learning via ERM

Our ERM learning method is closely related to that of Elliott and Lieli (2013) under the cohort design, where the celebrated maximum score estimator of Manski (1975, 1985) is adapted to accommodate class-specific utilities. We adopt the case-control design instead, with n_d independent replicates of \mathbf{X}_d observed: $\mathbf{X}_{d,[i]}$, $i = 1, \dots, n_d$, for $d = 0, 1$. Write $n \equiv n_0 + n_1$. The class-specific empirical risks and overall empirical risk are

$$\hat{\psi}_0(\mathbf{b}) = \hat{E}I(\mathbf{b}^\top \mathbf{X}_0^\circ > 0), \quad \hat{\psi}_1(\mathbf{b}) = \hat{E}I(\mathbf{b}^\top \mathbf{X}_1^\circ \leq 0), \quad \hat{\psi}(\mathbf{b}) = \omega\hat{\psi}_0(\mathbf{b}) + (1 - \omega)\hat{\psi}_1(\mathbf{b}),$$

where \hat{E} represents empirical average, e.g., $\hat{E}I(\mathbf{b}^\top \mathbf{X}_0^\circ > 0) = n_0^{-1} \sum_{i=1}^{n_0} I(\mathbf{b}^\top \mathbf{X}_{0,[i]}^\circ > 0)$.

ERM corresponds to the following optimization problem,

$$\min_{\mathbf{b}: \|\mathbf{b}\|_1=1} \hat{\psi}(\mathbf{b}), \tag{1}$$

and the estimated classifier $\widehat{\boldsymbol{\beta}}$ is a near minimizer, satisfying

$$\widehat{\psi}(\widehat{\boldsymbol{\beta}}) \leq \min_{\mathbf{b}: \|\mathbf{b}\|_1=1} \widehat{\psi}(\mathbf{b}) + \varepsilon_n, \quad \varepsilon_n = o(n^{-2/3}). \quad (2)$$

The classifier in Example 1 is a special case with $m = 1$.

The computation of problem (1) is challenging due to the non-convex, piecewise-constant objective function and the presence of an equality constraint. Huang and Sanda (2022) proposed a novel and effective algorithm tailored to this class of problems. The equality constraint is handled through a reformulation by incorporating a penalty term:

$$\min_{\mathbf{b}: \|\mathbf{b}\|_1 \leq 1} \widehat{\psi}(\mathbf{b}) - c\|\mathbf{b}\|_1, \quad (3)$$

for a constant $c > 0$. To address the non-smoothness, indicator function $I(x \leq 0)$ is approximated using $\sigma^{-1}\{(x - \sigma/2)^- - (x + \sigma/2)^-\}$, where $x^- \equiv -\min(x, 0)$ and $\sigma > 0$ is a smoothing parameter. This approximation also leads to a concave-convex decomposition of the objective function, enabling an application of the concave-convex procedure (Yuille and Rangarajan, 2003). Note that taking $c > 1$ in the smoothed problem ensures its minimizer bounded away from 0; see related discussion in Huang and Sanda (2022, section 4). The algorithm proceeds by solving a sequence of smoothed problems that converge to the original one, with decreasing σ values. More details are provided in Supplementary Appendix A.

2.2 Asymptotic theory on the ERM classifier

The ERM classifier is studied to provide a foundation for subsequent analyses of model risk prediction methods. Existing results for related estimators are extended and generalized. For the maximum score estimator, consistency (Manski, 1975, 1985) and weak convergence with cube-root asymptotics (Kim and Pollard, 1990) were established under a semiparametric quantile regression model. Elliott and Lieli (2013) considered a nonparametric model similar to ours, but established only consistency for their estimator.

Focus on consistency first, with the following regularity conditions.

Condition 1. (SAMPLE SIZES) As $n \rightarrow \infty$, n_1/n_0 converges to a finite constant $\gamma > 0$.

Condition 2. (IDENTIFIABILITY AND SEPARATION) The overall risk $\psi(\mathbf{b})$ and optimal classifier $\boldsymbol{\beta}$ satisfy $\psi(\boldsymbol{\beta}) < \inf_{\mathbf{b}: \|\mathbf{b}\|=1, \|\mathbf{b}-\boldsymbol{\beta}\|_1 \geq \varepsilon} \psi(\mathbf{b})$ for every $\varepsilon > 0$.

THEOREM 1. *Under Conditions 1–2, $\widehat{\boldsymbol{\beta}}$ converges to $\boldsymbol{\beta}$ almost surely, and $\widehat{\psi}(\widehat{\boldsymbol{\beta}})$ is strongly consistent for $\psi(\boldsymbol{\beta})$.*

This consistency result actually holds more generally, allowing $\varepsilon_n = o(1)$ instead in the definition (2) of $\widehat{\boldsymbol{\beta}}$.

Now, we establish weak convergence in the cube-root asymptotics framework of Kim and Pollard (1990). Several additional technical conditions are imposed. For a generic vector \mathbf{b} , write \mathbf{b}_ℓ as the ℓ -th element and $\mathbf{b}_{-\ell}$ as the vector with the ℓ -th element removed.

Condition 3. (DISTRIBUTION SMOOTHNESS) Two cases are considered based on the number of features: For $d = 0, 1$,

(A) $m = 1$: the density function of $\boldsymbol{\beta}^\top \mathbf{X}_d^\circ$ at 0 exists and is bounded;

(B) $m \geq 2$: there exists ℓ , $1 \leq \ell \leq m$, such that (i) $\boldsymbol{\beta}_\ell \neq 0$, (ii) $\mathbf{X}_{d,-\ell}$ is integrable, and

(iii) the conditional density function of $\boldsymbol{\beta}^\top \mathbf{X}_d^\circ \mid \mathbf{X}_{d,-\ell}$ exists and is bounded.

Since the classification is invariant under linear transformation of the features, Case (B) may be interpreted as corresponding to appropriately transformed features. As such, it is more general than it may initially appear.

Condition 4. (HESSIAN OF OVERALL RISK) The Hessian $\nabla^2 \psi(\mathbf{b})$ exists at $\mathbf{b} = \boldsymbol{\beta}$, and satisfies $\mathbf{h}^\top \nabla^2 \psi(\boldsymbol{\beta}) \mathbf{h} > 0$ for $\mathbf{h} \neq \mathbf{0}$ in the subspace orthogonal to $\boldsymbol{\beta}$.

Condition 5. (NONDEGENERACY OF LIMITING PROCESS) For $\mathbf{h} \neq \mathbf{0}$ in the subspace orthogonal to $\boldsymbol{\beta}$, $\mathbf{h}^\top \nabla \psi_d(\boldsymbol{\beta}) \neq 0$ for $d = 0, 1$.

Restricting \mathbf{h} to the subspace in Conditions 4–5 is linked to the scale invariance of the risks. These conditions are otherwise standard in M -estimation.

The limiting distribution of $\widehat{\boldsymbol{\beta}}$ is degenerate by definition. To avoid the complication, we focus on a related theoretical classifier instead, having its ℓ -th coefficient fixed to $\boldsymbol{\beta}_\ell$:

$$\check{\boldsymbol{\beta}} \equiv \begin{cases} \widehat{\boldsymbol{\beta}}\boldsymbol{\beta}_\ell/\widehat{\boldsymbol{\beta}}_\ell & \boldsymbol{\beta}_\ell\widehat{\boldsymbol{\beta}}_\ell > 0 \\ \boldsymbol{\beta} & \text{otherwise} \end{cases}.$$

Since $\widehat{\boldsymbol{\beta}}$ is consistent for $\boldsymbol{\beta}$, so is $\check{\boldsymbol{\beta}}$. Furthermore, with probability tending to 1, $\check{\boldsymbol{\beta}}$ is parallel to $\widehat{\boldsymbol{\beta}}$. Write $\phi_d(\mathbf{b}_{-\ell}) \equiv \psi_d(\mathbf{b})|_{\mathbf{b}_\ell=\boldsymbol{\beta}_\ell}$, $d = 0, 1$, $\phi(\mathbf{b}_{-\ell}) \equiv \psi(\mathbf{b})|_{\mathbf{b}_\ell=\boldsymbol{\beta}_\ell}$, and their empirical counterparts as $\widehat{\phi}_d(\mathbf{b}_{-\ell})$ and $\widehat{\phi}(\mathbf{b}_{-\ell})$, respectively. For asymptotic analysis, $\check{\boldsymbol{\beta}}_{-\ell}$ can be characterized as a near minimizer of an unconstrained problem:

$$\widehat{\phi}(\check{\boldsymbol{\beta}}_{-\ell}) \leq \min_{\mathbf{b}_{-\ell}} \widehat{\phi}(\mathbf{b}_{-\ell}) + o_p(n^{-2/3}).$$

However, $\check{\boldsymbol{\beta}}$ is not a practical classifier since the estimand $\boldsymbol{\beta}$ is involved.

Denote weak convergence by \rightsquigarrow .

THEOREM 2. *Suppose that Conditions 1–5 hold. Then,*

$$n^{2/3} \left\{ \begin{array}{c} \widehat{\phi}_0(\boldsymbol{\beta}_{-\ell} + n^{-1/3}\mathbf{s}) - \phi_0(\boldsymbol{\beta}_{-\ell} + n^{-1/3}\mathbf{s}) - \widehat{\phi}_0(\boldsymbol{\beta}_{-\ell}) + \phi_0(\boldsymbol{\beta}_{-\ell}) \\ \widehat{\phi}_1(\boldsymbol{\beta}_{-\ell} + n^{-1/3}\mathbf{s}) - \phi_1(\boldsymbol{\beta}_{-\ell} + n^{-1/3}\mathbf{s}) - \widehat{\phi}_1(\boldsymbol{\beta}_{-\ell}) + \phi_1(\boldsymbol{\beta}_{-\ell}) \\ \widehat{\phi}(\boldsymbol{\beta}_{-\ell} + n^{-1/3}\mathbf{s}) - \widehat{\phi}(\boldsymbol{\beta}_{-\ell}) \end{array} \right\} \rightsquigarrow \left\{ \begin{array}{c} W_0(\mathbf{s}) \\ W_1(\mathbf{s}) \\ Z(\mathbf{s}) \end{array} \right\}, \quad (4)$$

where $W_d(\mathbf{s})$, $d = 0, 1$, are two independent mean-zero Gaussian processes with continuous sample paths, and $Z(\mathbf{s}) = W(\mathbf{s}) + \mathbf{s}^\top \mathbf{H}\mathbf{s}/2$ for $W(\mathbf{s}) = \omega W_0(\mathbf{s}) + (1 - \omega)W_1(\mathbf{s})$ and $\mathbf{H} = \nabla^2 \phi(\boldsymbol{\beta}_{-\ell})$. Furthermore, $n^{1/3}(\check{\boldsymbol{\beta}}_{-\ell} - \boldsymbol{\beta}_{-\ell}) \rightsquigarrow \mathbf{U} \equiv \arg \min_{\mathbf{s}} Z(\mathbf{s})$.

Weak convergence of $\widehat{\boldsymbol{\beta}}$ follows immediately. Nevertheless, the results on $\check{\boldsymbol{\beta}}$ suffice for the risk prediction analysis of the estimated classifier, which is the primary focus of this article.

3. MODEL RISK PREDICTION

Over-optimism in empirical risk can be *exactly* characterized for simple models and certain loss functions, as exploited in classical correction methods (e.g., Efron, 2004). However,

such characterization becomes challenging for more complex predictive algorithms, including linear ERM classification. On the other hand, K -fold CV has rarely been analyzed with respect to the model prediction risk. A novel theoretical framework for assessing model risk prediction methods is therefore needed, which we develop based on higher-order asymptotics. We first elucidate the over-optimism in the empirical risk and the limitations of K -fold CV, which in turn motivate our proposed CAP procedure.

3.1 Asymptotic theory on empirical and K -fold CV risks

With estimated classifier $\widehat{\boldsymbol{\beta}}$, the overall model prediction risk is given by $\psi(\widehat{\boldsymbol{\beta}})$ and class-specific ones by $\psi_d(\widehat{\boldsymbol{\beta}})$, $d = 0, 1$. Building on the weak convergence results in Section 2.2, we obtain second-order expansions of the empirical risks to characterize the over-optimism through asymptotic bias (e.g., Shao, 2003, section 2.5.2).

THEOREM 3. *Under Conditions 1–5,*

$$n^{2/3}[\{\widehat{\psi}_d(\widehat{\boldsymbol{\beta}}) - \psi_d(\widehat{\boldsymbol{\beta}})\} - \{\widehat{\psi}_d(\boldsymbol{\beta}) - \psi_d(\boldsymbol{\beta})\}] \rightsquigarrow W_d(\mathbf{U}), \quad d = 0, 1, \quad (5)$$

$$n^{2/3}[\{\widehat{\psi}(\widehat{\boldsymbol{\beta}}) - \psi(\widehat{\boldsymbol{\beta}})\} - \{\widehat{\psi}(\boldsymbol{\beta}) - \psi(\boldsymbol{\beta})\}] \rightsquigarrow W(\mathbf{U}) = Z(\mathbf{U}) - \mathbf{U}^\top \mathbf{H} \mathbf{U} / 2, \quad (6)$$

where $W_d(\mathbf{U})$, $d = 0, 1$, have negative expectations, and $W(\mathbf{U})$ is negative almost surely.

Since $E\widehat{\psi}_d(\boldsymbol{\beta}) = \psi_d(\boldsymbol{\beta})$ and $E\widehat{\psi}(\boldsymbol{\beta}) = \psi(\boldsymbol{\beta})$, the empirical risks $\widehat{\psi}_d(\widehat{\boldsymbol{\beta}})$ and $\widehat{\psi}(\widehat{\boldsymbol{\beta}})$ are first-order asymptotically unbiased for the corresponding prediction risks $\psi_d(\widehat{\boldsymbol{\beta}})$ and $\psi(\widehat{\boldsymbol{\beta}})$. Similar first-order asymptotic results have been established previously (e.g., Dudoit and van der Laan, 2005), but they do not account for the observed poor performance of empirical risks. As a key and novel feature of our framework, the second-order asymptotic bias explains and characterizes the over-optimism. Although the over-optimism can be explained for the overall risk without resorting to asymptotics, this explanation is qualitative and does not extend to the class-specific risks.

With K -fold CV, the training data are randomly partitioned into K roughly equal-sized and non-overlapping folds, stratified by class. For each $k = 1, \dots, K$, let $\widehat{\boldsymbol{\beta}}^{(-k)}$ be the counterpart of $\widehat{\boldsymbol{\beta}}$ using the data except the k -th fold, $\widehat{\psi}_d^{(k)}(\mathbf{b})$ be the counterpart of $\widehat{\psi}_d(\mathbf{b})$ using the k -th fold only, for $d = 0, 1$. The CV class-specific and overall risks are given by

$$\overline{\psi}_{d,\text{cv}} = K^{-1} \sum_{k=1}^K \widehat{\psi}_d^{(k)}(\widehat{\boldsymbol{\beta}}^{(-k)}), \quad d = 0, 1, \quad \overline{\psi}_{\text{cv}} = \omega \overline{\psi}_{0,\text{cv}} + (1 - \omega) \overline{\psi}_{1,\text{cv}}, \quad (7)$$

respectively. Because of random splitting, $\widehat{\boldsymbol{\beta}}^{(-k)}$ is independent of $\widehat{\psi}_d^{(k)}(\mathbf{b})$. Thus, the CV risks are unbiased estimators of the CV ensemble prediction risks discussed in Section 1,

$$\psi_{d,\text{cv-ens}} \equiv K^{-1} \sum_{k=1}^K \psi_d(\widehat{\boldsymbol{\beta}}^{(-k)}), \quad d = 0, 1, \quad \psi_{\text{cv-ens}} \equiv K^{-1} \sum_{k=1}^K \psi(\widehat{\boldsymbol{\beta}}^{(-k)}),$$

respectively.

COROLLARY 1. *Suppose that $K \geq 2$ is fixed. Under Conditions 1–5,*

$$n^{2/3} \left[(\overline{\psi}_{d,\text{cv}} - \psi_{d,\text{cv-ens}}) - \{\widehat{\psi}_d(\boldsymbol{\beta}) - \psi_d(\boldsymbol{\beta})\} \right] \rightsquigarrow V_d, \quad d = 0, 1, \quad (8)$$

$$n^{2/3} \left[(\overline{\psi}_{\text{cv}} - \psi_{\text{cv-ens}}) - \{\widehat{\psi}(\boldsymbol{\beta}) - \psi(\boldsymbol{\beta})\} \right] \rightsquigarrow V, \quad (9)$$

$$n^{1/3} \left\{ \psi_{d,\text{cv-ens}} - \psi_d(\widehat{\boldsymbol{\beta}}) \right\} \rightsquigarrow S_d, \quad d = 0, 1, \quad (10)$$

$$n^{2/3} \left\{ \psi_{\text{cv-ens}} - \psi(\widehat{\boldsymbol{\beta}}) \right\} \rightsquigarrow S, \quad (11)$$

for some non-degenerate random variables V_d , V , S_d , and S , where V_d , V , and S_d have zero means and $ES = [\{(K - 1)/K\}^{-2/3} - 1]EU^\top \mathbf{H}U/2 > 0$.

The weak convergence results given by (8) and (9), with respect to the CV ensemble prediction risks, are not surprising. However, the CV ensemble prediction risks differ from the model prediction risks, as shown in (10) and (11), with the class-specific discrepancies in particular exhibiting a slower decay rate. Consequently, the CV estimator $\overline{\psi}_{d,\text{cv}}$ converges to $\psi_d(\widehat{\boldsymbol{\beta}})$ at a rate of order $n^{-1/3}$, slower than the empirical risk $\widehat{\psi}_d(\widehat{\boldsymbol{\beta}})$ of order $n^{-1/2}$ as given by Theorem 3. This result explains the observation in Example 1 that $\overline{\psi}_{d,\text{cv}}$ tracked $\psi_d(\widehat{\boldsymbol{\beta}})$

less accurately. For overall risk, the discrepancy is of order $n^{-2/3}$ and so the CV overall risk $\bar{\psi}_{\text{cv}}$ is first-order asymptotically equivalent to the empirical risk $\widehat{\psi}(\widehat{\boldsymbol{\beta}})$. Nevertheless, the CV overall risk exhibits a positive second-order bias, which decreases as K increases, and tends to be conservative in contrast to the empirical risk.

3.2 Proposed K -fold CAP

The theoretical results on the empirical risk and K -fold CV motivate a novel two-step model risk prediction method. The cross-audit step utilizes the same resampling scheme as K -fold CV to estimate the over-optimism in subsamples. Subsequently, the projection step accounts for the sample-size reduction to correct bias in the empirical risk.

The Cross-Audit Step. Write $\widehat{\psi}_d^{(-k)}(\mathbf{b})$ and $\widehat{\psi}^{(-k)}(\mathbf{b})$ as the counterparts of $\widehat{\psi}_d(\mathbf{b})$ and $\widehat{\psi}(\mathbf{b})$, respectively, using the data except the k -th fold, for $k = 1, \dots, K$ and $d = 0, 1$. Obtain K -fold empirical risks:

$$\bar{\psi}_{d,\text{emp}} = K^{-1} \sum_{i=1}^K \widehat{\psi}_d^{(-k)}(\widehat{\boldsymbol{\beta}}^{(-k)}), \quad d = 0, 1, \quad \bar{\psi}_{\text{emp}} = \omega \bar{\psi}_{0,\text{emp}} + (1 - \omega) \bar{\psi}_{1,\text{emp}}. \quad (12)$$

Their deviations from the K -fold CV counterparts, $\bar{\psi}_{d,\text{cv}}$ and $\bar{\psi}_{\text{cv}}$, provide bias estimates of empirical risks in the subsamples. As a consequence of ERM, $\bar{\psi}_{\text{emp}}$ and $\bar{\psi}_{\text{cv}}$ satisfy an inequality relationship.

PROPOSITION 1. Consider $\bar{\psi}_{\text{cv}}$ and $\bar{\psi}_{\text{emp}}$ defined in (7) and (12), respectively. Then,

$$\bar{\psi}_{\text{emp}} \leq \bar{\psi}_{\text{cv}} + (K - 1)\varepsilon_n,$$

where ε_n is the error tolerance in the definition (2) of the estimated classifier.

Thus, if ε_n is set to 0, the bias estimate of $\bar{\psi}_{\text{emp}}$ is nonpositive.

The Projection Step. As the subsamples are $(K - 1)/K$ of the full sample in size, the bias in $\bar{\psi}_{d,\text{emp}}$ is expected to be larger than that in $\widehat{\psi}_d(\widehat{\boldsymbol{\beta}})$. Shrink the bias estimate of $\bar{\psi}_{d,\text{emp}}$ by a factor of $\{(K - 1)/K\}^{2/3}$, to be consistent with the asymptotic bias of order $n^{-2/3}$ given

in Theorem 3:

$$\widehat{\psi}_{d,\text{cap}} = Q^{-1} \left[Q\{\widehat{\psi}_d(\widehat{\boldsymbol{\beta}})\} - \{(K-1)/K\}^{2/3} \{Q(\overline{\psi}_{d,\text{emp}}) - Q(\overline{\psi}_{d,\text{cv}})\} \right], \quad (13)$$

$$\widehat{\psi}_{\text{cap}} = \omega \widehat{\psi}_{0,\text{cap}} + (1-\omega) \widehat{\psi}_{1,\text{cap}}, \quad (14)$$

where $Q(\cdot)$ is a given monotone function. The choice of $Q(\cdot)$ is not essential asymptotically and could simply be, for example, the identity function. In our numerical studies, $Q(\cdot)$ was taken to be the standard normal quantile function for range preservation.

COROLLARY 2. *Suppose that K is fixed, and monotone function $Q(\cdot)$ is differentiable at $\psi_d(\boldsymbol{\beta})$, $d = 0, 1$, with non-zero derivatives. Under Conditions 1–5, $n^{2/3}[\{\widehat{\psi}_{d,\text{cap}} - \psi_d(\widehat{\boldsymbol{\beta}})\} - \{\widehat{\psi}_d(\boldsymbol{\beta}) - \psi_d(\boldsymbol{\beta})\}]$, $d = 0, 1$, and $n^{2/3}[\{\widehat{\psi}_{\text{cap}} - \psi(\widehat{\boldsymbol{\beta}})\} - \{\widehat{\psi}(\boldsymbol{\beta}) - \psi(\boldsymbol{\beta})\}]$ converge weakly to non-degenerate and mean-zero distributions.*

For overall risk prediction, the CAP estimator $\widehat{\psi}_{\text{cap}}$ is first-order asymptotically equivalent to both the empirical estimator $\widehat{\psi}(\widehat{\boldsymbol{\beta}})$ and the CV estimator $\overline{\psi}_{\text{cv}}$. However, the CAP estimator is second-order asymptotically unbiased, whereas the other two are not. Meanwhile, for class-specific risk prediction, the CAP estimator $\widehat{\psi}_{d,\text{cap}}$ and the empirical estimator $\widehat{\psi}_d(\widehat{\boldsymbol{\beta}})$ are first-order asymptotically equivalent, both converging faster than the CV estimator $\overline{\psi}_{d,\text{cv}}$. The class-specific CAP estimator remains second-order asymptotically unbiased.

REMARK 1. Model prediction risk is random because it depends on the training data, and its expectation is the *algorithm prediction risk*. Between the two estimands, existing estimators in the literature are often found to track the latter more closely despite that the former is typically of greater interest. In particular, CV estimators behave in this way in a number of settings; see Zhang (1995), Efron and Tibshirani (1997), Hastie, Tibshirani, and Friedman (2009), and Bates, Hastie and Tibshirani (2024). In contrast, the class-specific CAP risk estimator tracks the model prediction risk more closely because $\widehat{\psi}_{d,\text{cap}} - \psi_d(\widehat{\boldsymbol{\beta}}) = O_p(n^{-1/2})$ is dominated by the $n^{-1/3}$ -order variation of the model prediction risk $\psi_d(\widehat{\boldsymbol{\beta}})$. See Supplementary Appendix B for a numerical verification using Example 1.

REMARK 2. As an extension of K -fold CV, repeated K -fold CV has been suggested to stabilize estimation particularly for small samples (Burman, 1989). The same strategy applies to K -fold CAP. With the number of repetitions fixed, the asymptotic results in Corollaries 1–2 extends in a straightforward manner to repeated K -fold CV and CAP. In particular, repeated K -fold CAP preserves the same first-order asymptotics and second-order asymptotic unbiasedness.

REMARK 3. Unlike K -fold CV, K -fold CAP is largely insensitive to the choice of K . Corollary 2 shows that neither the first-order asymptotics nor the second-order asymptotic unbiasedness is affected. Smaller values of K offer computational advantages. Our numerical experience suggests that repeated 2-fold CAP with 16 repetitions performs well, which was the CAP method adopted in the simulation studies of Example 1.

REMARK 4. For computational convenience, classifiers are often constructed in practice using logistic regression (LR) for feature combination, followed by ERM for threshold estimation. The estimated combination coefficients typically converge at the faster parametric rate, even under model misspecification. Consequently, the resulting combination can be treated as a fixed single feature in model risk prediction of this LR-ERM classifier.

3.3 Inference with model risk bound

Following Corollary 2,

$$\begin{pmatrix} \hat{\psi}_{0,\text{cap}} \\ \hat{\psi}_{1,\text{cap}} \end{pmatrix} \sim \text{AN} \left\{ \begin{pmatrix} \psi_0(\hat{\boldsymbol{\beta}}) \\ \psi_1(\hat{\boldsymbol{\beta}}) \end{pmatrix}, \begin{pmatrix} \psi_0(\hat{\boldsymbol{\beta}})\{1 - \psi_0(\hat{\boldsymbol{\beta}})\}/n_0 & 0 \\ 0 & \psi_1(\hat{\boldsymbol{\beta}})\{1 - \psi_1(\hat{\boldsymbol{\beta}})\}/n_1 \end{pmatrix} \right\},$$

where AN denotes asymptotically normal. Marginally, the inference of class-specific risk $\psi_d(\hat{\boldsymbol{\beta}})$ is analogous to that of a binomial proportion. Among confidence intervals for a binomial proportion, the score interval (Wilson, 1927) is range-preserving and generally preferred (e.g., Agresti and Coull, 1998). We mimic this approach to derive a upper bound

for $\psi_d(\widehat{\beta})$, with nominal probability δ_d , as the larger solution q to

$$\frac{n_d(\widehat{\psi}_{d,\text{cap}} - q)^2}{q(1 - q)} = z_{\delta_d}^2,$$

where z_{δ_d} is the δ_d -quantile of the standard normal distribution. Because of the asymptotic independence, jointly the two class-specific risk bounds then have nominal probability $\delta_0\delta_1$.

For overall risk $\psi(\widehat{\beta})$, we propose an upper bound, with nominal probability δ , as the larger solution q to:

$$\min_{q_0, q_1: \omega q_0 + (1-\omega)q_1 = q} \frac{n_0(\widehat{\psi}_{0,\text{cap}} - q_0)^2}{q_0(1 - q_0)} + \frac{n_1(\widehat{\psi}_{1,\text{cap}} - q_1)^2}{q_1(1 - q_1)} = z_{\delta}^2,$$

on the basis of quadratic inference function (e.g., Lindsay and Qu, 2003).

The preceding risk inference is first-order asymptotically justified. Although this justification remains valid when the empirical risks are used instead in the procedure, performance may deteriorate due to their substantial bias. On the other hand, it is unclear how to construct a suitable inference procedure based on K -fold CV, even for the overall risk, despite the fact that the K -fold CV overall risk point estimator is first-order asymptotically equivalent to its K -fold CAP counterpart.

4. NUMERICAL STUDIES

Simulations were conducted to evaluate linear ERM classification and model risk prediction methods for both ERM and LR-ERM classifiers. For illustration, we also present an application to breast cancer detection. The algorithmic implementation of linear ERM classification is detailed in Supplementary Appendix A.

4.1 Simulations

We considered the same set-ups as in Huang and Sanda (2022). In all of them, features in class 0 were independent and identically distributed as standard normal, whereas those in class 1 followed distributions that varied across set-ups. Either three or six features were

considered. For the former, all the features were informative as their class 1 distributions differed from standard normal. In the latter case, three additional independent noninformative features were included, each in class 1 following the standard normal distribution. Four class 1 distributions for the three informative features were formulated, mimicking cancer detection applications:

Scenario A: independent and identically distributed as normal with mean 0.9 and variance 1;

Scenario B: independent and normally distributed with the same mean of 0.8 but different variances of 0.5, 1, and 2;

Scenario C: normally distributed with the same mean of 1, different variances of 0.5, 1, and 2, and pairwise correlation coefficient of 0.5;

Scenario D: mixture of two distributions each with the three features being independent and normally distributed, one with probability 2/3 having means of 1.7, 1.7, and 0 and variances of 0.5, 2, and 1, and the other with probability 1/3 having means of 0, 0, and 1.7 and the same variance of 1.

In the first three scenarios, class 1 features differed in their dependence structure and variability. In contrast, Scenario D emulated cancer heterogeneity, with two subtypes associated with elevations in the first two features and the last feature separately. The overall risk used $\omega = 0.25$, and the optimal classifiers yielded class-specific risks of (0.47, 0.069), (0.54, 0.052), (0.57, 0.045), and (0.48, 0.072) for classes 0 and 1 under Scenarios A–D, respectively. The class sizes were set equal, $n_0 = n_1$, ranging from 100 to 500. Results were based on 1000 simulated datasets for each set-up.

The main focus was on linear ERM classification. Our algorithm proved both effective and efficient, and the estimated classifier behaved in accordance with the asymptotic theory; see Supplementary Appendix C. For the model risk prediction, Tables 1 and 2 report results for repeated 2-fold CAP with 16 repetitions along with empirical risk estimation, the bootstrap method of Harrell, Lee, and Mark (1996) with 100 resamples, and 10-fold CV, for settings

Table 1: Simulation results on overall | class 0 | class 1 risk prediction of the ERM classifier with three features

| n_0 | empirical | | | bootstrap | | | 10-fold CV | | | repeated 2-fold CAP | | |
|---------|-------------|----------|-------------|-----------|--------|----------|------------|----------|----------------|---------------------|---|---|
| | B | D | C | B | D | C | B | D | C | B | D | C |
| $= n_1$ | | | | | | | | | | | | |
| | Scenario A | | | | | | | | | | | |
| 100 | -38 -42 -36 | 38 51 38 | -14 -16 -13 | 22 40 24 | 1 -4 3 | 23 51 30 | -2 -3 -2 | 20 39 24 | 94.4 94.9 94.0 | | | |
| 200 | -25 -25 -25 | 26 34 26 | -8 -8 -8 | 15 28 17 | 0 -2 1 | 16 38 21 | -1 0 -1 | 13 27 16 | 93.9 95.9 93.1 | | | |
| 300 | -20 -20 -20 | 20 28 21 | -6 -7 -6 | 12 24 13 | 0 0 0 | 13 33 17 | -1 -1 -1 | 11 22 12 | 94.4 94.6 93.9 | | | |
| 400 | -17 -18 -16 | 17 24 17 | -5 -5 -5 | 10 20 11 | 0 -2 1 | 10 29 14 | -1 -1 -1 | 10 20 11 | 94.6 94.4 95.0 | | | |
| 500 | -14 -14 -14 | 15 21 15 | -5 -5 -5 | 9 18 10 | 1 0 1 | 9 26 13 | 0 0 -1 | 8 18 9 | 94.3 95.6 95.0 | | | |
| | Scenario B | | | | | | | | | | | |
| 100 | -36 -37 -35 | 36 48 36 | -13 -15 -13 | 21 41 22 | 0 -5 2 | 21 51 27 | -2 0 -2 | 20 39 23 | 92.0 95.5 93.3 | | | |
| 200 | -24 -23 -25 | 25 33 26 | -8 -7 -8 | 14 28 15 | 1 -1 2 | 16 37 19 | -2 1 -2 | 14 28 16 | 92.6 95.0 91.7 | | | |
| 300 | -19 -19 -19 | 19 27 20 | -6 -6 -6 | 11 23 12 | 0 0 0 | 12 31 15 | -1 -1 -1 | 11 23 12 | 94.6 94.8 93.9 | | | |
| 400 | -16 -16 -15 | 16 23 16 | -5 -5 -5 | 10 20 10 | 1 -2 1 | 10 28 13 | -1 -2 -1 | 9 19 10 | 94.4 94.2 94.5 | | | |
| 500 | -14 -13 -14 | 14 21 14 | -4 -4 -4 | 8 18 9 | 1 0 1 | 9 25 11 | -1 -1 -1 | 8 18 9 | 93.5 94.3 94.7 | | | |
| | Scenario C | | | | | | | | | | | |
| 100 | -37 -44 -34 | 37 53 36 | -12 -14 -12 | 22 40 24 | 0 -1 0 | 24 52 30 | -3 -3 -2 | 20 40 24 | 94.9 94.9 93.7 | | | |
| 200 | -24 -27 -23 | 24 35 24 | -6 -6 -6 | 14 28 15 | 1 -3 2 | 16 41 21 | -2 -1 -2 | 14 29 16 | 93.5 94.2 94.1 | | | |
| 300 | -18 -19 -17 | 18 28 18 | -4 -4 -4 | 11 23 12 | 1 -1 2 | 12 35 17 | -1 0 -2 | 11 23 12 | 93.9 95.0 94.4 | | | |
| 400 | -14 -16 -14 | 15 23 15 | -4 -3 -4 | 10 20 11 | 1 -3 2 | 11 30 15 | -1 0 -1 | 9 20 10 | 94.1 95.0 94.4 | | | |
| 500 | -13 -14 -12 | 14 21 14 | -3 -3 -3 | 8 18 9 | 1 -2 2 | 9 29 13 | -1 0 -1 | 9 18 10 | 94.9 94.2 92.6 | | | |
| | Scenario D | | | | | | | | | | | |
| 100 | -40 -33 -42 | 40 46 43 | -13 -10 -15 | 23 40 26 | 2 0 3 | 24 54 31 | -2 1 -3 | 22 38 27 | 93.7 95.6 92.2 | | | |
| 200 | -26 -22 -27 | 26 31 28 | -9 -7 -9 | 16 28 18 | 1 -3 2 | 16 41 21 | -1 0 -1 | 14 27 17 | 94.3 95.4 94.7 | | | |
| 300 | -20 -17 -21 | 21 27 22 | -6 -5 -7 | 12 23 14 | 0 -2 1 | 13 32 17 | -1 -1 -1 | 12 23 13 | 94.0 94.4 94.5 | | | |
| 400 | -17 -14 -18 | 18 23 19 | -5 -5 -5 | 10 20 12 | 1 0 1 | 11 28 15 | -1 0 -1 | 10 20 11 | 93.9 94.5 94.3 | | | |
| 500 | -15 -12 -16 | 15 21 16 | -4 -4 -4 | 9 18 10 | 1 0 1 | 10 28 14 | -1 0 -1 | 9 18 10 | 94.7 95.4 94.9 | | | |

B: bias ($\times 1000$), D: mean absolute deviation ($\times 1000$), C: coverage probability of 95% risk bound (%).

Table 2: Simulation results on overall | class 0 | class 1 risk prediction of the ERM classifier with six features

| n_0 | empirical | | | bootstrap | | | 10-fold CV | | | repeated 2-fold CAP | | | | | | | | | | | | | | | | | |
|---------|------------|-----|-----|-----------|----|----|------------|-----|-----|---------------------|----|----|---|----|----|----|----|----|----|----|----|----|----|----|------|------|------|
| | B | D | C | B | D | C | B | D | C | B | D | C | | | | | | | | | | | | | | | |
| $= n_1$ | | | | | | | | | | | | | | | | | | | | | | | | | | | |
| | Scenario A | | | | | | | | | | | | | | | | | | | | | | | | | | |
| 100 | -59 | -63 | -57 | 59 | 67 | 58 | -23 | -20 | -24 | 28 | 43 | 31 | 0 | -8 | 3 | 25 | 52 | 31 | -5 | -1 | -6 | 24 | 41 | 29 | 89.2 | 93.5 | 88.2 |
| 200 | -39 | -41 | -38 | 39 | 45 | 38 | -13 | -13 | -13 | 17 | 30 | 19 | 0 | -2 | 1 | 17 | 37 | 21 | -3 | -1 | -3 | 15 | 29 | 17 | 91.9 | 93.5 | 92.3 |
| 300 | -30 | -31 | -30 | 30 | 34 | 30 | -10 | -10 | -9 | 13 | 24 | 15 | 0 | 1 | 10 | 12 | 33 | 17 | -2 | 0 | -3 | 12 | 23 | 14 | 92.7 | 94.2 | 92.6 |
| 400 | -25 | -26 | -24 | 25 | 30 | 25 | -8 | -7 | -8 | 12 | 21 | 13 | 0 | -2 | 1 | 11 | 27 | 15 | -1 | -1 | -1 | 10 | 20 | 12 | 92.4 | 94.4 | 93.3 |
| 500 | -20 | -21 | -20 | 20 | 24 | 21 | -7 | -6 | -7 | 10 | 18 | 11 | 1 | 0 | 1 | 9 | 26 | 13 | 0 | 1 | 0 | 8 | 17 | 9 | 95.8 | 95.7 | 95.0 |
| | Scenario B | | | | | | | | | | | | | | | | | | | | | | | | | | |
| 100 | -57 | -59 | -57 | 58 | 65 | 57 | -22 | -19 | -22 | 27 | 44 | 29 | 2 | -5 | 4 | 24 | 50 | 31 | -6 | 0 | -8 | 24 | 41 | 29 | 87.2 | 93.5 | 86.5 |
| 200 | -37 | -38 | -37 | 37 | 43 | 37 | -13 | -11 | -13 | 17 | 31 | 18 | 1 | 1 | 11 | 16 | 37 | 20 | -3 | -1 | -4 | 15 | 28 | 17 | 90.8 | 94.2 | 91.5 |
| 300 | -29 | -28 | -30 | 29 | 32 | 30 | -9 | -9 | -9 | 13 | 24 | 14 | 0 | 0 | 0 | 12 | 32 | 16 | -3 | 1 | -4 | 11 | 24 | 13 | 92.9 | 94.4 | 92.4 |
| 400 | -24 | -24 | -23 | 24 | 28 | 24 | -7 | -6 | -8 | 11 | 21 | 12 | 0 | -1 | 1 | 11 | 28 | 14 | -1 | 0 | -2 | 9 | 20 | 11 | 93.5 | 94.9 | 92.9 |
| 500 | -19 | -19 | -20 | 20 | 23 | 20 | -7 | -5 | -7 | 10 | 18 | 10 | 1 | -1 | 1 | 9 | 24 | 12 | 0 | 1 | 0 | 8 | 17 | 9 | 94.3 | 95.9 | 95.1 |
| | Scenario C | | | | | | | | | | | | | | | | | | | | | | | | | | |
| 100 | -58 | -66 | -56 | 58 | 70 | 56 | -21 | -19 | -21 | 26 | 43 | 28 | 2 | -1 | 3 | 25 | 55 | 33 | -6 | -2 | -8 | 24 | 40 | 29 | 90.8 | 94.8 | 89.5 |
| 200 | -37 | -40 | -36 | 37 | 44 | 36 | -12 | -12 | -11 | 17 | 30 | 18 | 1 | -2 | 2 | 17 | 40 | 23 | -3 | 1 | -4 | 16 | 28 | 18 | 90.9 | 94.6 | 90.7 |
| 300 | -27 | -30 | -27 | 28 | 34 | 27 | -9 | -9 | -10 | 13 | 24 | 14 | 1 | -1 | 2 | 12 | 33 | 17 | -2 | 1 | -3 | 12 | 24 | 13 | 93.8 | 94.1 | 92.5 |
| 400 | -23 | -24 | -22 | 23 | 28 | 23 | -7 | -7 | -7 | 11 | 21 | 12 | 0 | -2 | 0 | 11 | 30 | 16 | -1 | 2 | -2 | 9 | 20 | 11 | 94.9 | 95.0 | 93.5 |
| 500 | -20 | -21 | -19 | 20 | 25 | 20 | -5 | -5 | -5 | 9 | 18 | 10 | 0 | -1 | 1 | 10 | 27 | 14 | -1 | 1 | -2 | 9 | 18 | 10 | 94.5 | 95.0 | 93.5 |
| | Scenario D | | | | | | | | | | | | | | | | | | | | | | | | | | |
| 100 | -59 | -56 | -61 | 59 | 62 | 61 | -24 | -20 | -25 | 29 | 44 | 32 | 2 | -1 | 2 | 25 | 53 | 32 | -4 | 2 | -7 | 24 | 39 | 29 | 90.4 | 94.8 | 88.6 |
| 200 | -38 | -34 | -40 | 39 | 40 | 40 | -13 | -9 | -14 | 18 | 28 | 20 | 0 | -3 | 1 | 17 | 38 | 23 | -2 | 3 | -4 | 16 | 29 | 18 | 93.3 | 96.1 | 91.9 |
| 300 | -31 | -29 | -32 | 31 | 32 | 32 | -9 | -9 | -10 | 14 | 24 | 15 | 0 | -3 | 1 | 13 | 34 | 18 | -2 | 0 | -3 | 12 | 22 | 14 | 93.3 | 95.1 | 94.4 |
| 400 | -25 | -24 | -26 | 25 | 28 | 26 | -8 | -8 | -8 | 12 | 21 | 14 | 0 | 0 | 0 | 12 | 29 | 16 | -1 | 0 | -2 | 10 | 20 | 12 | 93.1 | 94.9 | 92.8 |
| 500 | -21 | -20 | -22 | 21 | 24 | 22 | -7 | -5 | -7 | 10 | 18 | 11 | 1 | 0 | 1 | 10 | 26 | 14 | 0 | 0 | 0 | 9 | 18 | 11 | 94.6 | 94.5 | 95.4 |

B: bias ($\times 1000$), D: mean absolute deviation ($\times 1000$), C: coverage probability of 95% risk bound (%).

with three and six features, respectively. As expected, the empirical estimator exhibited substantial over-optimism for both overall and class-specific risks. The bootstrap estimator reduced this bias but remained overly optimistic. In contrast, 10-fold CV exhibited negligible bias. While the mean absolute deviation of 10-fold CV for overall risk was smaller than that of the empirical estimator and comparable to that of the bootstrap estimator, this pattern did not extend to class-specific risks, particularly with larger sample sizes, mirroring the phenomenon observed in Example 1. By comparison, repeated 2-fold CAP outperformed the alternatives for both overall and class-specific risk in terms of bias and mean absolute deviation. Moreover, its risk bound had coverage close to the nominal level, especially as the sample size increased. Additional results on repeated 2-fold CV, repeated 10-fold CV, and repeated 10-fold CAP further confirmed the superior performance of K -fold CAP in general and its relative insensitivity to the choice of K ; see Supplementary Appendix C. Simulations for the model risk prediction of LR-ERM classification, which is more commonly used in practice (Remark 4), showed similar performance patterns; see Supplementary Appendix D.

4.2 *Application to breast cancer detection*

For illustration, we analyzed a clinical study for breast cancer detection using demographic variables and routine blood measurements (Patricio et al., 2018). The Breast Cancer Coimbra dataset (Patricio et al., 2018) consists of 64 women with breast cancer and 52 healthy volunteers. The features considered were glucose, resistin, age, and BMI; all were log-transformed. To prioritize accurate classification of cancer cases, we set $\omega = 0.25$.

Table 3 reports the ERM and LR-ERM classifiers together with their estimated model prediction risks. The two classifiers differed considerably. Although LR-ERM classifier is often used for computational convenience, it can be less predictive than ERM classifier under model misspecification. Indeed, the CAP risk estimates, along with the 95% risk bounds, suggested improved performance of the ERM classifier. The four point prediction risk estimates were broadly consistent with the patterns observed in the simulation studies.

5. DISCUSSION

In this article, we have developed K -fold CAP, a novel and theoretically justified method for model risk prediction. Like classical analytic correction methods, it aims to correct the over-optimism of empirical risk, but does so via a K -fold CV-style resampling scheme informed by asymptotic theory. For concreteness, the exposition has focused on linear ERM classification. Nevertheless, K -fold CAP applies generally to prediction algorithms involving cube-root asymptotics. The generalization can be made even more broadly, by matching the shrinking factor in the projection step with the order of the leading asymptotic bias of the empirical risk. For most problems amenable to classical analytic correction methods, including prediction likelihood targeted by AIC, the bias is of order n^{-1} leading to a shrinking factor of $(K - 1)/K$. However, the asymptotic bias for many modern and complex prediction algorithms remains poorly understood, which merits further investigation.

A fully automatic procedure that does not require asymptotic analysis would be desirable. However, the asymptotic bias, which typically arises in second-order asymptotics, may not have its order reliably estimated from the data. Nevertheless, K -fold CAP can adopt a *working* shrinking factor. Although second-order asymptotic unbiasedness is no longer

Table 3: ERM and LR-ERM classifications for breast cancer detection

| | ERM | LR-ERM | | ERM | | | LR-ERM | | |
|---------------|-----------------------|--------|------|-----------------------|-------|-------|---------|-------|-------|
| | estimated classifiers | | | model risk prediction | | | | | |
| | | | | overall | HL | BC | overall | HL | BC |
| threshold | 0.436 | 0.661 | emp | 0.148 | 0.500 | 0.031 | 0.173 | 0.365 | 0.109 |
| log(glucose) | 0.273 | 0.207 | boot | 0.192 | 0.580 | 0.063 | 0.203 | 0.418 | 0.131 |
| log(resistin) | 0.052 | 0.031 | CV | 0.233 | 0.558 | 0.125 | 0.214 | 0.481 | 0.125 |
| log(age) | -0.145 | -0.012 | CAP | 0.217 | 0.612 | 0.085 | 0.223 | 0.429 | 0.154 |
| log(BMI) | -0.093 | -0.088 | RB | 0.278 | 0.715 | 0.161 | 0.294 | 0.542 | 0.242 |

emp: empirical estimation, boot: bootstrap of Harrell et al. with 100 re-samples, CV: 10-fold CV, CAP: repeated 2-fold CAP with 16 repetitions, RB: 95% risk bound.
 HL: healthy volunteer, BC: breast cancer.

guaranteed, the procedure still possesses theoretical advantages over K -fold CV and could achieve a substantial bias reduction. Suppose that the over-optimism decays no faster than order n^{-1} , as faster decay would make it less consequential. If we adopt a working shrinking factor of $\{(K - 1)/K\}^{1/2}$, then 10-fold CAP incurs a second-order asymptotic bias within $1 - (9/10)^{\pm 1/2} \approx \pm 5\%$ of that of the empirical risk.

While model prediction risk is often targeted in practice, other notions of prediction risk may also be of interest, particularly algorithm prediction risk; see Remark 1. Defined as the expectation of model prediction risk, it reflects the performance of the learning algorithm rather than a specific learned model; see Dietterich (1998) for a detailed discussion of prediction estimands and their practical implications. K -fold CV has been used to estimate algorithm prediction risk, with its variance studied for uncertainty quantification (Nadeau and Bengio, 2003; Bengio and Grandvalet, 2004; Markatou et al., 2005). Our results suggest that K -fold CAP may also offer advantages for this purpose. Further investigation, along with the development of the associated inferential procedures, is an important direction for future work.

APPENDIX: PROOFS

Proof of Theorem 1

Under Condition 1, almost surely

$$\sup_{\mathbf{b}} |\widehat{\psi}_d(\mathbf{b}) - \psi_d(\mathbf{b})| = o(1), \quad d = 0, 1,$$

since $\{I(\mathbf{b}^\top \mathbf{X}_0^\circ > 0) : \mathbf{b} \in \mathbb{R}^{m+1}\}$ and $\{I(\mathbf{b}^\top \mathbf{X}_1^\circ \leq 0) : \mathbf{b} \in \mathbb{R}^{m+1}\}$ are Donsker classes (e.g., Kosorok, 2008, lemma 9.12) and thus also Glivenko–Cantelli classes. Subsequently,

$$\sup_{\mathbf{b}} |\widehat{\psi}(\mathbf{b}) - \psi(\mathbf{b})| = o(1),$$

almost surely. Therefore, $\widehat{\psi}(\widehat{\boldsymbol{\beta}}) - \psi(\widehat{\boldsymbol{\beta}}) = o(1)$ and $\widehat{\psi}(\boldsymbol{\beta}) - \psi(\boldsymbol{\beta}) = o(1)$, almost surely. They, together with $\widehat{\psi}(\widehat{\boldsymbol{\beta}}) \leq \widehat{\psi}(\boldsymbol{\beta}) + o(1)$ implied by display (2), give $\psi(\widehat{\boldsymbol{\beta}}) \leq \psi(\boldsymbol{\beta}) + o(1)$ almost

surely. Under Condition 2, the strong consistency of $\widehat{\boldsymbol{\beta}}$ then follows standard M -estimation arguments (e.g., van der Vaart, 1998, proof of theorem 5.7).

Proof of Theorem 2

The proof follows the general cube-root asymptotics framework of Kim and Pollard (1990), with two adaptations for our problem, the case-control design and minimization formulation.

Write

$$g(\mathbf{x}^\circ; \mathbf{b}_{-\ell}) = I(\mathbf{b}_{-\ell}^\top \mathbf{x}_{-\ell}^\circ + \boldsymbol{\beta}_\ell \mathbf{x}_\ell^\circ \leq 0) - I(\boldsymbol{\beta}^\top \mathbf{x}^\circ \leq 0).$$

Note that $\widehat{\phi}_d(\mathbf{b}_{-\ell}) - \widehat{\phi}_d(\boldsymbol{\beta}_{-\ell}) = (-1)^{d+1} \widehat{E}g(\mathbf{X}_d^\circ; \mathbf{b}_{-\ell})$, for $d = 0, 1$. The class of functions,

$$\mathcal{G}_\varepsilon = \{g(\cdot; \mathbf{b}_{-\ell}) : \|\mathbf{b}_{-\ell} - \boldsymbol{\beta}_{-\ell}\|_\infty \leq \varepsilon\},$$

has envelope

$$\begin{aligned} G_\varepsilon(\mathbf{x}^\circ) &= \sup_{\|\mathbf{b}_{-\ell} - \boldsymbol{\beta}_{-\ell}\|_\infty \leq \varepsilon} |g(\mathbf{x}^\circ; \mathbf{b}_{-\ell})| \\ &= I \left\{ \min_{\|\mathbf{b}_{-\ell} - \boldsymbol{\beta}_{-\ell}\|_\infty \leq \varepsilon} (\boldsymbol{\beta}_{-\ell} - \mathbf{b}_{-\ell})^\top \mathbf{x}_{-\ell}^\circ < \boldsymbol{\beta}^\top \mathbf{x}^\circ \leq \max_{\|\mathbf{b}_{-\ell} - \boldsymbol{\beta}_{-\ell}\|_\infty \leq \varepsilon} (\boldsymbol{\beta}_{-\ell} - \mathbf{b}_{-\ell})^\top \mathbf{x}_{-\ell}^\circ \right\}. \end{aligned}$$

Since the subgraphs of functions in \mathcal{G}_∞ form a VC class with bounded $G_\varepsilon(\mathbf{x}^\circ)$, \mathcal{G}_ε is uniformly manageable (Kim and Pollard, 1990, section 3).

We now check the remaining regularity conditions of the main theorem in Kim and Pollard (1990), except for trivial ones due to bounded $g(\mathbf{x}^\circ; \mathbf{b}_{-\ell})$ and $G_\varepsilon(\mathbf{x}^\circ)$ in our problem.

Condition 4 implies that $\nabla^2 \phi(\boldsymbol{\beta}_{-\ell})$ exists. Meanwhile,

$$\begin{aligned} V_d(\mathbf{s}, \mathbf{t}) &= \lim_{\alpha \rightarrow \infty} \alpha E \{g(\mathbf{X}_d^\circ; \boldsymbol{\beta}_{-\ell} + \mathbf{s}/\alpha) g(\mathbf{X}_d^\circ; \boldsymbol{\beta}_{-\ell} + \mathbf{t}/\alpha)\} \\ &= \begin{cases} E \{ \min(|\mathbf{s}^\top \mathbf{X}_{d,-\ell}^\circ|, |\mathbf{t}^\top \mathbf{X}_{d,-\ell}^\circ|) f_{\boldsymbol{\beta}^\top \mathbf{X}_d^\circ}(0) I(\mathbf{s}^\top \mathbf{X}_{d,-\ell}^\circ \mathbf{t}^\top \mathbf{X}_{d,-\ell}^\circ > 0) \} & m = 1 \\ EE \{ \min(|\mathbf{s}^\top \mathbf{X}_{d,-\ell}^\circ|, |\mathbf{t}^\top \mathbf{X}_{d,-\ell}^\circ|) f_{\boldsymbol{\beta}^\top \mathbf{X}_d^\circ | \mathbf{X}_{d,-\ell}}(0) \\ \quad \times I(\mathbf{s}^\top \mathbf{X}_{d,-\ell}^\circ \mathbf{t}^\top \mathbf{X}_{d,-\ell}^\circ > 0) \mid \mathbf{X}_{d,-\ell} \} & m \geq 2 \end{cases}, \end{aligned}$$

exists under Condition 3. Above, $f_{\boldsymbol{\beta}^\top \mathbf{X}_d^\circ}$ is the density function of $\boldsymbol{\beta}^\top \mathbf{X}_d^\circ$, and $f_{\boldsymbol{\beta}^\top \mathbf{X}_d^\circ | \mathbf{X}_{d,-\ell}}$ is the conditional counterpart given $\mathbf{X}_{d,-\ell}$.

Next, we show $EG_\varepsilon(\mathbf{X}_d^\circ)^2 = EG_\varepsilon(\mathbf{X}_d^\circ) = O(\varepsilon)$ as $\varepsilon \downarrow 0$, under Condition 3. This is obvious in the case of $m = 1$. For $m \geq 2$,

$$\begin{aligned}
EG_\varepsilon(\mathbf{X}_d^\circ) &= EE\{G_\varepsilon(\mathbf{X}_d^\circ) \mid \mathbf{X}_{d,-\ell}\} \\
&= E\{F_{\beta^\top \mathbf{X}_d^\circ \mid \mathbf{X}_{d,-\ell}}(\varepsilon \|\mathbf{X}_{d,-\ell}^\circ\|_1) - F_{\beta^\top \mathbf{X}_d^\circ \mid \mathbf{X}_{d,-\ell}}(-\varepsilon \|\mathbf{X}_{d,-\ell}^\circ\|_1)\} \\
&= 2\varepsilon E\{f_{\beta^\top \mathbf{X}_d^\circ \mid \mathbf{X}_{d,-\ell}}(\varepsilon^* \|\mathbf{X}_{d,-\ell}^\circ\|_1) \|\mathbf{X}_{d,-\ell}^\circ\|_1\} \\
&= O(\varepsilon),
\end{aligned}$$

where $F_{\beta^\top \mathbf{X}_d^\circ \mid \mathbf{X}_{d,-\ell}}$ is the conditional distribution function of $\beta^\top \mathbf{X}_d^\circ$ given $\mathbf{X}_{d,-\ell}$ and $\varepsilon^* \in [-\varepsilon, \varepsilon]$. Similar arguments can be used to establish $E|g(\mathbf{X}_d^\circ; \mathbf{b}_{-\ell}) - g(\mathbf{X}_d^\circ; \mathbf{b}_{-\ell}^*)| = O(\|\mathbf{b}_{-\ell} - \mathbf{b}_{-\ell}^*\|_\infty)$ for $\mathbf{b}_{-\ell}$ and $\mathbf{b}_{-\ell}^*$ near $\beta_{-\ell}$.

Then, the assertion on the weak convergence of $\hat{\phi}_d(\cdot)$ and $\hat{\phi}(\cdot)$ follows the main theorem of Kim and Pollard (1990). Furthermore, $\nabla^2 \phi(\beta_{-\ell})$ is positive definite under Condition 4. Meanwhile, the covariance kernel of process $W(\cdot)$, as given by $V(\mathbf{s}, \mathbf{t}) = \omega^2 V_0(\mathbf{s}, \mathbf{t}) + (1 - \omega)^2 V_1(\mathbf{s}, \mathbf{t})$, satisfies

$$V(\mathbf{s}, \mathbf{s}) - 2V(\mathbf{s}, \mathbf{t}) + V(\mathbf{t}, \mathbf{t}) = V(\mathbf{s} - \mathbf{t}, \mathbf{s} - \mathbf{t}).$$

Then, Gaussian process $Z(\cdot)$ has nondegenerate increments since $V(\mathbf{s}, \mathbf{s}) = \omega^2 |\mathbf{s}^\top \nabla \phi_0(\beta_{-\ell})| + (1 - \omega)^2 |\mathbf{s}^\top \nabla \phi_1(\beta_{-\ell})| \neq 0$ for $\mathbf{s} \neq \mathbf{0}$ under Condition 5. The weak convergence of $\check{\beta}_{-\ell}$ subsequently follows.

Proof of Theorem 3

Following the proof of the argmax continuous mapping theorem in Kim and Pollard (1990, theorem 2.7), we invoke the almost sure representation theorem of Dudley for the weak convergence result in (4) such that the counterparts in a new probability space sharing the same distributions have almost sure convergence in the sense of Kim and Pollard (1990,

section 2.2):

$$n^{2/3} \left\{ \begin{array}{l} \tilde{\phi}_0(\boldsymbol{\beta}_{-\ell} + n^{-1/3}\mathbf{s}) - \phi_0(\boldsymbol{\beta}_{-\ell} + n^{-1/3}\mathbf{s}) - \tilde{\phi}_0(\boldsymbol{\beta}_{-\ell}) + \phi_0(\boldsymbol{\beta}_{-\ell}) \\ \tilde{\phi}_1(\boldsymbol{\beta}_{-\ell} + n^{-1/3}\mathbf{s}) - \phi_1(\boldsymbol{\beta}_{-\ell} + n^{-1/3}\mathbf{s}) - \tilde{\phi}_1(\boldsymbol{\beta}_{-\ell}) + \phi_1(\boldsymbol{\beta}_{-\ell}) \\ \tilde{\phi}(\boldsymbol{\beta}_{-\ell} + n^{-1/3}\mathbf{s}) - \tilde{\phi}(\boldsymbol{\beta}_{-\ell}) \end{array} \right\} \rightarrow \left\{ \begin{array}{l} \widetilde{W}_0(\mathbf{s}) \\ \widetilde{W}_1(\mathbf{s}) \\ \widetilde{Z}(\mathbf{s}) \end{array} \right\},$$

almost surely. Meanwhile, the processes on the left-hand side are stochastically equicontinuous (Kim and Pollard, 1990, lemma 4.6). Write $\widetilde{\boldsymbol{\beta}}_{-\ell}$ and $\widetilde{\mathbf{U}}$ as the counterparts of $\check{\boldsymbol{\beta}}_{-\ell}$ and \mathbf{U} , respectively. Similar to Kim and Pollard (1990, proof of theorem 2.7), it can be established that

$$\widetilde{\Pr}^* \{ \|n^{1/3}(\widetilde{\boldsymbol{\beta}}_{-\ell} - \boldsymbol{\beta}_{-\ell}) - \widetilde{\mathbf{U}}\|_2 > \varepsilon \} \rightarrow 0$$

for each $\varepsilon > 0$, where $\widetilde{\Pr}^*$ denotes the outer probability. Then, it follows that

$$\widetilde{\Pr}^* \{ |n^{2/3}[\{\tilde{\phi}_d(\widetilde{\boldsymbol{\beta}}_{-\ell}) - \phi_d(\widetilde{\boldsymbol{\beta}}_{-\ell})\} - \{\tilde{\phi}_d(\boldsymbol{\beta}_{-\ell}) - \phi_d(\boldsymbol{\beta}_{-\ell})\}] - \widetilde{W}_d(\widetilde{\mathbf{U}})| > \varepsilon \} \rightarrow 0, \quad d = 0, 1,$$

for each $\varepsilon > 0$. Thus,

$$\begin{aligned} n^{2/3}[\{\widehat{\phi}_d(\check{\boldsymbol{\beta}}_{-\ell}) - \phi_d(\check{\boldsymbol{\beta}}_{-\ell})\} - \{\widehat{\phi}_d(\boldsymbol{\beta}_{-\ell}) - \phi_d(\boldsymbol{\beta}_{-\ell})\}] &\rightsquigarrow W_d(\mathbf{U}), \quad d = 0, 1, \\ n^{2/3}[\{\widehat{\phi}(\check{\boldsymbol{\beta}}_{-\ell}) - \phi(\check{\boldsymbol{\beta}}_{-\ell})\} - \{\widehat{\phi}(\boldsymbol{\beta}_{-\ell}) - \phi(\boldsymbol{\beta}_{-\ell})\}] &\rightsquigarrow W(\mathbf{U}). \end{aligned}$$

Convergence results in (5)–(6) then follow, as $\widehat{\phi}_d(\check{\boldsymbol{\beta}}_{-\ell}) = \widehat{\psi}_d(\widehat{\boldsymbol{\beta}})$ and $\phi_d(\check{\boldsymbol{\beta}}_{-\ell}) = \psi_d(\widehat{\boldsymbol{\beta}})$ with probability tending to 1.

Next, we establish that \mathbf{U} possesses finite moments of all orders, and $EW(\mathbf{U})$ exists. Define a norm $\|\mathbf{s}\| \equiv (\mathbf{s}^\top \mathbf{H}\mathbf{s}/2)^{1/2}$ for vector \mathbf{s} . We shall exploit the rescaling property of $W(\mathbf{s})$, that is, $W(c\mathbf{s})$ having the same distribution as $c^{1/2}W(\mathbf{s})$ for any $c > 0$. From Shi, Lu, and Song (2018, lemma A.2), we have $\Pr\{\inf_{\|\mathbf{s}\| \leq 1} Z(\mathbf{s}) \leq -x\} = O\{\exp(-x)\}$ as $x \rightarrow \infty$. It follows $\Pr\{\inf_{\|\mathbf{s}\| \leq 1} W(\mathbf{s}) \leq -x\} \leq c \exp(-x)$ for some constant $c > 0$, when x is sufficiently large. Taking such an $x \geq 2$, we have

$$\begin{aligned} \Pr(\|\mathbf{U}\| > x) &\leq \Pr\{\inf_{\|\mathbf{s}\| > x} Z(\mathbf{s}) \leq 0\} \\ &\leq \sum_{j=1}^{\infty} \Pr\{\inf_{\|\mathbf{s}\| \in (x+j-1, x+j]} W(\mathbf{s}) + \|\mathbf{s}\|^2 \leq 0\} \end{aligned}$$

$$\begin{aligned}
&\leq \sum_{j=1}^{\infty} \Pr \left[\inf_{\|\mathbf{s}\| \leq 1} W\{(x+j)\mathbf{s}\} \leq -(x+j-1)^2 \right] \\
&= \sum_{j=1}^{\infty} \Pr \left\{ \inf_{\|\mathbf{s}\| \leq 1} W(\mathbf{s}) \leq -(x+j-1)^2(x+j)^{-1/2} \right\} \\
&\leq \sum_{j=1}^{\infty} \Pr \left\{ \inf_{\|\mathbf{s}\| \leq 1} W(\mathbf{s}) \leq -x-j+1 \right\} \\
&\leq \sum_{j=1}^{\infty} c \exp(-x-j+1) \\
&= ce(e-1)^{-1} \exp(-x).
\end{aligned}$$

Thus, \mathbf{U} has finite moments of all orders. Subsequently, the existence of $EW(\mathbf{U})$ follows from that of $EZ(\mathbf{U})$ by Shi, Lu, and Song (2018, lemma A.2).

Now, introduce $Z_d(\mathbf{s}) = \omega^{1-d}(1-\omega)^d W_d(\mathbf{s}) + \|\mathbf{s}\|^2$ and $\mathbf{U}_d = \arg \min_{\mathbf{s}} Z_d(\mathbf{s})$, for $d = 0, 1$. Since $EZ_d(\mathbf{U}_d)$ exists and $Z_d(\mathbf{U}_d) \leq Z_d(\mathbf{U})$, $EZ_d(\mathbf{U})$ exists. Subsequently, $EW_d(\mathbf{U})$ exists. Similarly, $EW_d(\mathbf{U}_{1-d})$ exists. Since \mathbf{U}_{1-d} is independent of process $W_d(\cdot)$, $EW_d(\mathbf{U}_{1-d}) = 0$. From $Z(\mathbf{U}) \leq Z(\mathbf{U}_0)$, we have

$$\omega W_0(\mathbf{U}) + (1-\omega)W_1(\mathbf{U}) + \|\mathbf{U}\|^2 \leq \omega W_0(\mathbf{U}_0) + (1-\omega)W_1(\mathbf{U}_0) + \|\mathbf{U}_0\|^2.$$

Upon taking expectations on both sides, we obtain

$$(1-\omega)EW_1(\mathbf{U}) \leq E\{Z_0(\mathbf{U}_0) - Z_0(\mathbf{U})\}.$$

Since $\Pr(\mathbf{U} = \mathbf{U}_0) = 0$ as can be shown, $EW_1(\mathbf{U}) < 0$. Similarly, $EW_0(\mathbf{U}) < 0$.

Proof of Corollary 1

For each class, the fold sizes differ by at most 1, which does not affect the asymptotic results. Without loss of generality, we assume that both n_0 and n_1 are divisible by K so that the K folds have equal sizes.

Write $\widehat{\phi}_d^{(k)}(\mathbf{b}_{-\ell})$ and $\widehat{\phi}_d^{(-k)}(\mathbf{b}_{-\ell})$ as the counterparts of $\widehat{\phi}_d(\mathbf{b}_{-\ell})$ using data of the k -th fold and data except the k -th fold, respectively, for $k = 1, \dots, K$ and $d = 0, 1$. Extending Theorem 2 to address subsets from the K -fold partition, we obtain

$$\left\{ (n/K)^{2/3} [\widehat{\phi}_d^{(k)}\{\boldsymbol{\beta}_{-\ell} + (n/K)^{-1/3}\mathbf{s}\} - \phi_d\{\boldsymbol{\beta}_{-\ell} + (n/K)^{-1/3}\mathbf{s}\} - \widehat{\phi}_d^{(k)}(\boldsymbol{\beta}_{-\ell}) + \phi_d(\boldsymbol{\beta}_{-\ell})], \right.$$

$$\begin{aligned}
& \{(K-1)n/K\}^{2/3} \{\widehat{\phi}_d^{(-k)}[\boldsymbol{\beta}_{-\ell} + \{(K-1)n/K\}^{-1/3} \mathbf{s}] \\
& \quad - \phi_d[\boldsymbol{\beta}_{-\ell} + \{(K-1)n/K\}^{-1/3} \mathbf{s}] - \widehat{\phi}_d^{(-k)}(\boldsymbol{\beta}_{-\ell}) + \phi_d(\boldsymbol{\beta}_{-\ell})\}, \\
& n^{2/3} \{\widehat{\phi}_d(\boldsymbol{\beta}_{-\ell} + n^{-1/3} \mathbf{s}) - \phi_d(\boldsymbol{\beta}_{-\ell} + n^{-1/3} \mathbf{s}) - \widehat{\phi}_d(\boldsymbol{\beta}_{-\ell}) + \phi_d(\boldsymbol{\beta}_{-\ell})\} : d = 0, 1; k = 1, \dots, K \} \\
& \rightsquigarrow \left\{ W_d^{(k)}(\mathbf{s}), W_d^{(-k)}(\mathbf{s}), W_d(\mathbf{s}) : d = 0, 1; k = 1, \dots, K \right\},
\end{aligned}$$

where Gaussian processes $W_d^{(k)}(\cdot)$, $d = 0, 1$, $k = 1, \dots, K$, are independent of each other, $W_d^{(-k)}(\mathbf{s}) = (K-1)^{-1/3} \sum_{l \neq k} W_d^{(l)}\{(K-1)^{-1/3} \mathbf{s}\}$, and $W_d(\mathbf{s}) = K^{-1/3} \sum_{k=1}^K W_d^{(k)}(K^{-1/3} \mathbf{s})$. For each $d = 0, 1$, $W_d^{(k)}(\cdot)$, $W_d^{(-k)}(\cdot)$, and $W_d(\cdot)$ have the same distribution. Let $W^{(-k)}(\mathbf{s}) = \omega W_0^{(-k)}(\mathbf{s}) + (1-\omega) W_1^{(-k)}(\mathbf{s})$, $Z^{(-k)}(\mathbf{s}) = W^{(-k)}(\mathbf{s}) + \mathbf{s}^\top \mathbf{H} \mathbf{s} / 2$, and $\mathbf{U}^{(-k)} = \arg \min_{\mathbf{s}} Z^{(-k)}(\mathbf{s})$.

Then, using the techniques in the proof of Theorem 3, we can show results (8) and (9) with $V_d = K^{-1/3} \sum_{k=1}^K W_d^{(k)}\{(K-1)^{-1/3} \mathbf{U}^{(-k)}\}$ and $V = \omega V_0 + (1-\omega) V_1$. Since $W_d^{(k)}(\cdot)$ is independent of $\mathbf{U}^{(-k)}$, $EV_d = EV = 0$. Results (10) and (11) follow from a generalized version of the Delta method, with

$$\begin{aligned}
S_d &= \mathbf{D}_d^\top [\{(K-1)/K\}^{-1/3} K^{-1} \sum_{k=1}^K \mathbf{U}^{(-k)} - \mathbf{U}], \\
S &= \{(K-1)/K\}^{-2/3} K^{-1} \sum_{k=1}^K \mathbf{U}^{(-k)\top} \mathbf{H} \mathbf{U}^{(-k)} / 2 - \mathbf{U}^\top \mathbf{H} \mathbf{U} / 2,
\end{aligned}$$

where $\mathbf{D}_d = \nabla \phi_d(\boldsymbol{\beta}_{-\ell})$. Meanwhile, S_d is non-degenerate as

$$S_d = \{(K-1)/K\}^{-1/3} \mathbf{D}_d^\top \left\{ K^{-1} \sum_{k=1}^K \arg \min_{\mathbf{s}} Z^{(-k)}(\mathbf{s}) - \arg \min_{\mathbf{s}} K^{-1} \sum_{k=1}^K Z^{(-k)}(\mathbf{s}) \right\}$$

and $\arg \min$ is not a linear operator. The expectations of S_d and S follow from $E\mathbf{U} = \mathbf{0}$ and $\mathbf{U}^{(-k)}$ has the same distribution as \mathbf{U} .

Proof of Proposition 1

Since $\widehat{\psi}^{(-k)}(\widehat{\boldsymbol{\beta}}^{(-k)}) \leq \min_{\mathbf{b}: \|\mathbf{b}\|_1=1} \widehat{\psi}^{(-k)}(\mathbf{b}) + \varepsilon_n$,

$$(K-1) \sum_{k=1}^K \widehat{\psi}^{(-k)}(\widehat{\boldsymbol{\beta}}^{(-k)}) - K(K-1)\varepsilon_n \leq \sum_{k=1}^K \sum_{l \neq k} \widehat{\psi}^{(-k)}(\widehat{\boldsymbol{\beta}}^{(-l)})$$

$$\begin{aligned}
&= \sum_{k=1}^K \sum_{l \neq k} \widehat{\psi}^{(-l)}(\widehat{\boldsymbol{\beta}}^{(-k)}) \\
&= \sum_{k=1}^K \widehat{\psi}^{(k)}(\widehat{\boldsymbol{\beta}}^{(-k)}) + \sum_{k=1}^K \frac{K-2}{K-1} \sum_{l \neq k} \widehat{\psi}^{(l)}(\widehat{\boldsymbol{\beta}}^{(-k)}) \\
&= \sum_{k=1}^K \left\{ \widehat{\psi}^{(k)}(\widehat{\boldsymbol{\beta}}^{(-k)}) + (K-2)\widehat{\psi}^{(-k)}(\widehat{\boldsymbol{\beta}}^{(-k)}) \right\}.
\end{aligned}$$

Thus,

$$\sum_{k=1}^K \widehat{\psi}^{(-k)}(\widehat{\boldsymbol{\beta}}^{(-k)}) \leq \sum_{k=1}^K \widehat{\psi}^{(k)}(\widehat{\boldsymbol{\beta}}^{(-k)}) + K(K-1)\varepsilon_n,$$

and the assertion follows.

Proof of Corollary 2

Following the proof of Corollary 1,

$$n^{2/3}[\{\bar{\psi}_{d,\text{emp}} - \psi_{d,\text{cv-ens}}\} - \{\widehat{\psi}_d(\boldsymbol{\beta}) - \psi_d(\boldsymbol{\beta})\}] \rightsquigarrow \{(K-1)/K\}^{-2/3} K^{-1} \sum_{k=1}^K W_d^{(-k)}(\mathbf{U}^{(-k)}),$$

for $d = 0, 1$. It holds jointly with result (8), leading to

$$n^{2/3}(\bar{\psi}_{d,\text{emp}} - \bar{\psi}_{d,\text{cv}}) \rightsquigarrow \{(K-1)/K\}^{-2/3} K^{-1} \sum_{k=1}^K W_d^{(-k)}(\mathbf{U}^{(-k)}) - V_d.$$

Since $Q(\cdot)$ is differentiable at $\psi_d(\boldsymbol{\beta})$,

$$Q(\bar{\psi}_{d,\text{emp}}) - Q(\bar{\psi}_{d,\text{cv}}) = Q'\{\psi_d(\boldsymbol{\beta})\}(\bar{\psi}_{d,\text{emp}} - \bar{\psi}_{d,\text{cv}}) + o_p(n^{-2/3}).$$

Similarly, $Q^{-1}(\cdot)$ is differentiable at $Q\{\psi_d(\boldsymbol{\beta})\}$ and we have

$$\widehat{\psi}_{d,\text{cap}} = \widehat{\psi}_d(\widehat{\boldsymbol{\beta}}) - \{(K-1)/K\}^{2/3}(\bar{\psi}_{d,\text{emp}} - \bar{\psi}_{d,\text{cv}}) + o_p(n^{-2/3}).$$

In light of result (5), we obtain

$$n^{2/3}[\{\widehat{\psi}_{d,\text{cap}} - \psi_d(\widehat{\boldsymbol{\beta}})\} - \{\widehat{\psi}_d(\boldsymbol{\beta}) - \psi_d(\boldsymbol{\beta})\}] \rightsquigarrow W_d(\mathbf{U}) - K^{-1} \sum_{k=1}^K W_d^{(-k)}(\mathbf{U}^{(-k)}) + \{(K-1)/K\}^{2/3} V_d.$$

Accordingly, for the overall risk,

$$n^{2/3}[\{\widehat{\psi}_{\text{cap}} - \psi(\widehat{\boldsymbol{\beta}})\} - \{\widehat{\psi}(\boldsymbol{\beta}) - \psi(\boldsymbol{\beta})\}] \rightsquigarrow W(\mathbf{U}) - K^{-1} \sum_{k=1}^K W^{(-k)}(\mathbf{U}^{(-k)}) + \{(K-1)/K\}^{2/3} V.$$

The assertions follow as $W_d^{(-k)}(\mathbf{U}^{(-k)})$ and $W^{(-k)}(\mathbf{U}^{(-k)})$ have the same distributions as $W_d(\mathbf{U})$ and $W(\mathbf{U})$, respectively.

SUPPLEMENTARY MATERIALS

Computational algorithm for linear ERM classification, additional simulation results of Example 1, additional simulation results of ERM classification in Section 4.1, and simulation results of LR-ERM classification.

FUNDING

This research was partially supported by the National Institutes of Health grants R01 CA230268, R01 CA283687, and P30 AI050409.

REFERENCES

- Agresti, A. and Coull, B. A. (1998), “Approximate Is Better Than “Exact” for Interval Estimation of Binomial Proportions,” *The American Statistician*, 52, 119–126.
- Akaike, H. (1974), “A New Look at the Statistical Model Identification,” *IEEE Transactions on Automatic Control*, 19, 716–723.
- Allen, D. M. (1974), “The Relationship Between Variable Selection and Data Augmentation and a Method for Prediction,” *Technometrics*, 16, 125–127.
- Austern, M. and Zhou, W. (2020), “Asymptotics of Cross-Validation,” arXiv preprint. arXiv:2001.11111.
- Bates, S., Hastie, T. and Tibshirani, R. (2024), “Cross-Validation: What Does It Estimate and How Well Does It Do It?” *Journal of the American Statistical Association*, 119, 1434–1445.
- Bayle, P., Bayle, A., Mackey, L. and Janson, L. (2020), “Cross-Validation Confidence Intervals for Test Error,” *NIPS’20: Proceedings of the 34th International Conference on Neural Information Processing Systems*, 16339–16350.

- Bengio, Y. and Grandvalet, Y. (2004), “No Unbiased Estimator of the Variance of k-Fold Cross-Validation,” *Journal of Machine Learning Research*, 5, 1089–1105.
- Benkeser, D., Petersen, M. and van der Laan, M. J. (2020), “Improved Small-Sample Estimation of Nonlinear Cross-Validated Prediction Metrics,” *Journal of the American Statistical Association*, 115, 1917–1932.
- Burman, P. (1989), “A Comparative Study of Ordinary Cross-Validation, v -Fold Cross-Validation, and the Repeated Learning-Testing Methods,” *Biometrika*, 76, 503–514.
- Dietterich, T. G. (1998), “Approximate Statistical Tests for Comparing Supervised Classification Learning Algorithms,” *Neural Computation*, 10, 1895–1923.
- Dudoit, S. and van der Laan, M. J. (2005), “Asymptotics of Cross-Validated Risk Estimation in Estimator Selection and Performance Assessment,” *Statistical Methodology*, 2, 131–154.
- Efron, B. (1983), “Estimating the Error Rate of a Prediction Rule: Improvement on Cross-Validation,” *Journal of the American Statistical Association*, 78, 316–331.
- Efron, B. (2004), “The Estimation of Prediction Error (With Discussion),” *Journal of the American Statistical Association*, 99, 619–632.
- Efron, B. and Tibshirani, R. (1997), “Improvements on Cross-Validation: The .632+ Bootstrap Method,” *Journal of the American Statistical Association*, 92, 548–560.
- Elliott, G. and Lieli, R. P. (2013), “Predicting Binary Outcomes,” *Journal of Econometrics*, 174, 15–26.
- Geisser, S. (1975), “The Predictive Sample Reuse Method With Applications,” *Journal of the American Statistical Association*, 70, 320–328.

- Harrell, F. E., Lee, K. L., and Mark, D. B. (1996), “Multivariable Prognostic Models: Issues in Developing Models, Evaluating Assumptions and Adequacy, and Measuring and Reducing Errors,” *Statistics in Medicine*, 15, 361–387.
- Hastie, T., Tibshirani, R., and Friedman, J. (2009), *The Elements of Statistical Learning: Data Mining, Inference, and Prediction*, Springer: New York.
- Huang, Y. and Sanda, M. G. (2022), “Linear Biomarker Combination for Constrained Classification,” *The Annals of Statistics*, 50, 2793–2815.
- Kim, J. and Pollard, D. (1990), “Cube Root Asymptotics,” *The Annals of Statistics*, 18, 191–219.
- Kosorok, M. R. (2008), *Introduction to Empirical Processes and Semiparametric Inference*, Springer: New York.
- LeDell, E., Petersen, M. and van der Laan, M. (2015), “Computationally Efficient Confidence Intervals for Cross-Validated Area under the ROC Curve Estimates,” *Electronic Journal of Statistics*, 9, 1583–1607.
- Lindsay, B. and Qu, A. (2003), “Inference Functions and Quadratic Score Tests,” *Statistical Science*, 18, 394–410.
- Mallows, C. L. (1973), “Some Comments on C_p ,” *Technometrics*, 15, 661–675.
- Manski, C. F. (1975), “Maximum Score Estimation of the Stochastic Utility Model of Choice,” *Journal of Econometrics*, 3, 205–228.
- Manski, C. F. (1985), “Semiparametric Analysis of Discrete Response: Asymptotic Properties of the Maximum Score Estimator,” *Journal of Econometrics*, 27, 313–333.

- Markatou, M., Tian, H., Biswas, S. and Hripcsak, G. (2005), “Analysis of Variance of Cross-Validation Estimators of the Generalization Error,” *Journal of Machine Learning Research*, 6, 1127–1168.
- Nadeau, C. and Bengio, Y. (2003), “Inference for the Generalization Error,” *Machine Learning*, 52, 239–281.
- Patricio, M., Pereira, J., Crisostomo, J. et al. (2018), “Using Resistin, Glucose, Age, and BMI to Predict the Presence of Breast Cancer,” *BMC Cancer*, 18:29.
- Patricio, M., Pereira, J., Crisostomo, J. et al. (2018), “Breast Cancer Coimbra Dataset,” *UCI Machine Learning Repository*, University of California, Irvine. Available at <https://archive.ics.uci.edu/dataset/451/breast+cancer+coimbra>.
- Shao, J. (2003), *Mathematical Statistics*, 2nd ed, Springer: New York.
- Shi, C., Lu, W. and Song, R. (2018). “A Massive Data Framework for M-Estimators With Cubic-Rate,” *Journal of the American Statistical Association*, 113, 1698–1709.
- Stein, C. M. (1981), “Estimation of the Mean of a Multivariate Normal Distribution,” *The Annals of Statistics*, 9, 1135–1151.
- Stone, M. (1974), “Cross-Validatory Choice and Assessment of Statistical Predictions,” *Journal of the Royal Statistical Society Series B*, 36, 111–147.
- Stone, M. (1977), “An Asymptotic Equivalence of Choice of Model by Cross-Validation and Akaike’s Criterion,” *Journal of the Royal Statistical Society Series B*, 39, 44–47.
- van der Vaart, A. W. (1998), *Asymptotic Statistics*, Cambridge University Press.
- Wilson, E. B. (1927), “Probable Inference, the Law of Succession, and Statistical Inference,” *Journal of the American Statistical Association*, 22, 209–212.

Yuille, A. L. and Rangarajan, A. (2003), “The Concave-Convex Procedure,” *Neural Computation*, 15, 915–936.

Zhang, P. (1995), “Assessing Prediction Error in Non-parametric Regression,” *Scandinavian Journal of Statistics*, 22, 83–94.

Supplementary Appendix

Cross-Audit Projection for Model Risk Prediction

Yijian HUANG

A COMPUTATIONAL ALGORITHM FOR LINEAR ERM CLASSIFICATION

Upon replacing $I(x \leq 0)$ with $\sigma^{-1}\{(x - \sigma/2)^- - (x + \sigma/2)^-\}$, problem (3) becomes

$$\begin{aligned} \min_{\mathbf{b}: \|\mathbf{b}\|_1 \leq 1} \quad & \sigma^{-1} \widehat{E} \{ \omega(-\mathbf{b}^\top \mathbf{X}_0^\circ - \sigma/2)^- + (1 - \omega)(\mathbf{b}^\top \mathbf{X}_1^\circ - \sigma/2)^- \} \\ & - \left[\sigma^{-1} \widehat{E} \{ \omega(-\mathbf{b}^\top \mathbf{X}_0^\circ + \sigma/2)^- + (1 - \omega)(\mathbf{b}^\top \mathbf{X}_1^\circ + \sigma/2)^- \} + c\|\mathbf{b}\|_1 \right]. \end{aligned} \quad (\text{S1})$$

For a fixed σ , the concave-convex procedure (Yuille and Rangarajan, 2003) is applied for the optimization, which is the core of Algorithm S1. At each step, the concave component of the

Algorithm S1: Pseudo code for linear ERM classification

Input: initial value \mathbf{b}_0 of \mathbf{b} , starting value of σ , shrinking factor of σ

Output: optimizer for \mathbf{b}

$i \leftarrow 0$.

repeat

repeat /* Concave-convex procedure with fixed σ : problem (S1) */

1. *Convexify.* Form

$$\begin{aligned} T(\mathbf{b}, t; \mathbf{b}_i, t_i) \equiv & \sigma^{-1} \widehat{E} \{ \omega(-\mathbf{b}_i^\top \mathbf{X}_0^\circ + \sigma/2)^- + (1 - \omega)(\mathbf{b}_i^\top \mathbf{X}_1^\circ + \sigma/2)^- \} \\ & + \sigma^{-1} \widehat{E} \{ -\omega(\mathbf{b} - \mathbf{b}_i)^\top \mathbf{X}_0^\circ I(\mathbf{b}_i^\top \mathbf{X}_0^\circ \geq \sigma/2) \\ & \quad + (1 - \omega)(\mathbf{b} - \mathbf{b}_i)^\top \mathbf{X}_1^\circ I(\mathbf{b}_i^\top \mathbf{X}_1^\circ \leq -\sigma/2) \} \\ & + c\|\mathbf{b}_i\|_1 + c \text{sign}(\mathbf{b}_i)^\top (\mathbf{b} - \mathbf{b}_i). \end{aligned}$$

2. *Solve.* Set the value of \mathbf{b}_{i+1} to the solution of

$$\begin{aligned} \min_{\mathbf{b}: \|\mathbf{b}\|_1 \leq 1} \quad & \sigma^{-1} \widehat{E} \{ \omega(-\mathbf{b}^\top \mathbf{X}_0^\circ - \sigma/2)^- + (1 - \omega)(\mathbf{b}^\top \mathbf{X}_1^\circ - \sigma/2)^- \} \\ & - T(\mathbf{b}, t; \mathbf{b}_i, t_i) \end{aligned} \quad (\text{S2})$$

3. *Update iteration.* $i \leftarrow i + 1$.

until sufficiently small improvement in objective function of problem (S1).

Shrink σ value by the given factor.

until sufficiently small improvement in objective function of problem (3).

objective function is replaced with its tangent plane at the current coefficient value resulting in a linear program given by (S2). Problem (S1) is only an approximation of problem (3). A sequence of decreasing σ values are taken in the outer loop of Algorithm S1.

For the numerical studies in Section 4, the algorithm was implemented using a linear programming solver from the R package `Rmosek`. The LR-ERM classifier was used for initialization. The initial value of σ was set to the larger of the two class-specific maximum gaps between adjacent order statistics of the initial combinations. The shrinking factor for the σ sequence was set to 0.8, and the constant c in problem (3) was taken to be 2.

B ADDITIONAL SIMULATION RESULTS OF EXAMPLE 1

Figure S1 presents scatter plots of the CAP estimates against the model prediction risks, along with the corresponding correlation coefficients. For overall risk, the CAP estimator had a weak correlation with the model prediction risk. In contrast, for class-specific risks, strong correlations were observed demonstrating that the CAP estimators tracked the model prediction risks more closely than the algorithm prediction risks; see Remark 1.

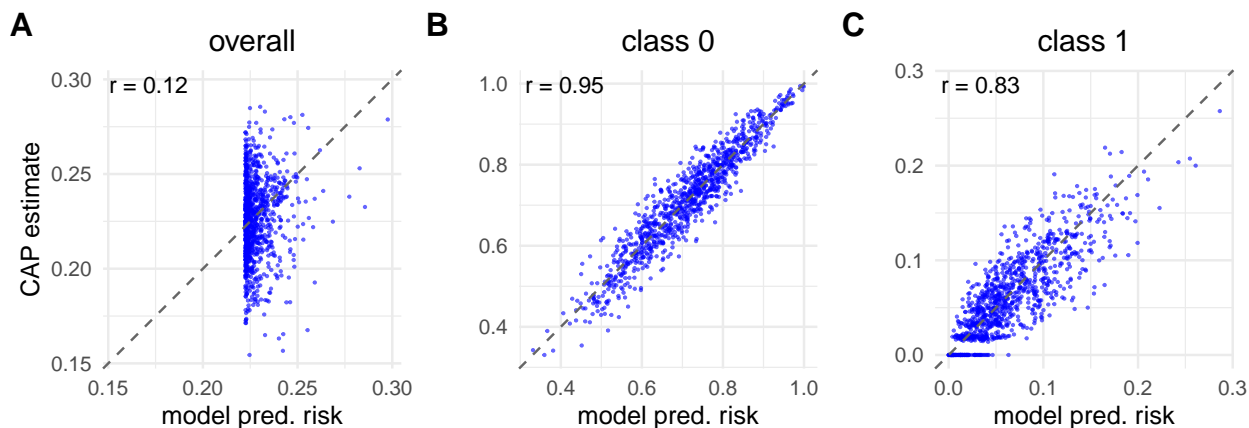


Figure S1: Simulation results on CAP estimates versus model prediction risks in single-feature ERM binary classification with $X_0 \sim N(0, 1)$, $X_1 \sim N(1, 1)$, $\omega = 0.25$, and $n_0 = n_1 = 100$, based on 1000 simulated datasets.

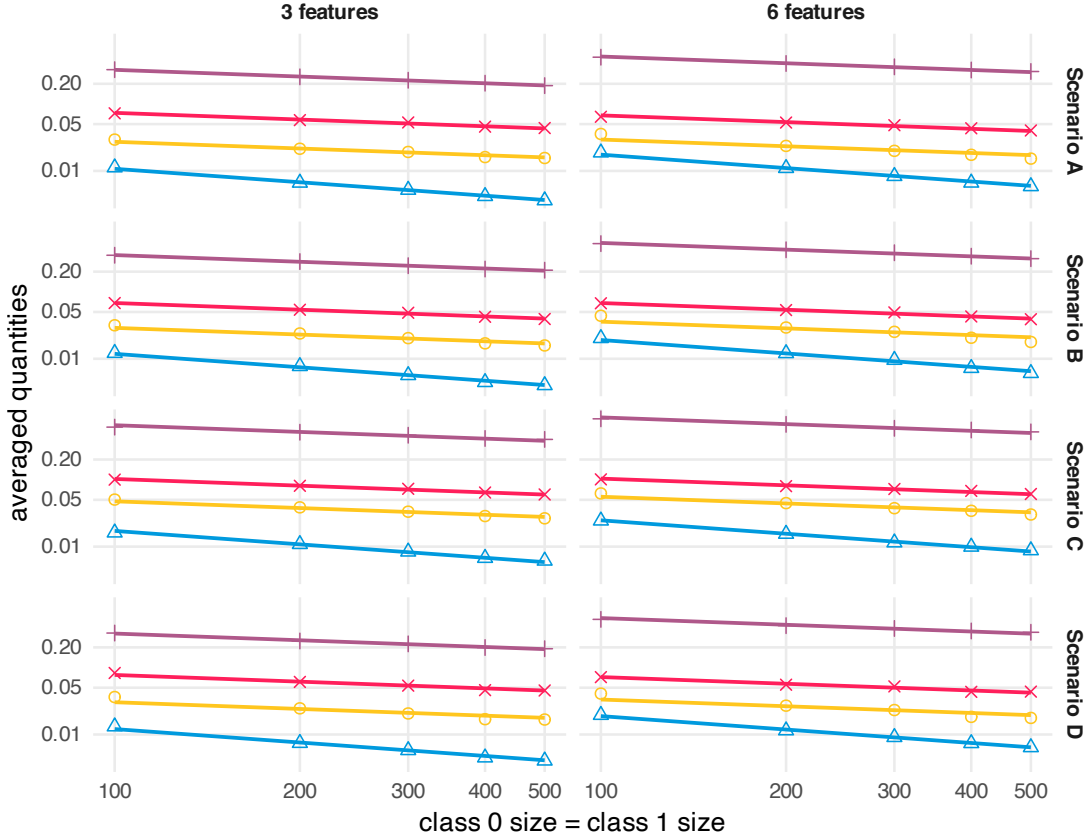


Figure S2: Simulation results on $\|\hat{\beta} - \beta\|_1$ (+), $\psi(\beta) - \psi(\hat{\beta})$ (Δ), $|\psi_0(\beta) - \psi_0(\hat{\beta})|$ (\times), and $|\psi_1(\beta) - \psi_1(\hat{\beta})|$ (\circ). Each straight line is the least-squares fitting of an averaged quantity versus sample size, both on the logarithmic scale, with the slope fixed to $-2/3$ for $\psi(\beta) - \psi(\hat{\beta})$ and to $-1/3$ for others.

C ADDITIONAL SIMULATION RESULTS OF ERM CLASSIFICATION IN SECTION 4.1

Figure S2 shows mean absolute error of $\hat{\beta}$ and mean absolute differences between model prediction risks and the risks of the optimal classifier. Across all set-ups, mean $\psi(\beta) - \psi(\hat{\beta})$ diminished with the sample size at an approximate rate of $n^{-2/3}$, whereas the others exhibited a rate of about $n^{-1/3}$. These findings corroborate the asymptotic results of cube-root convergence of $\hat{\beta}$.

Tables S1 and S2 present simulation results for additional model risk prediction methods, repeated 2-fold CV, repeated 10-fold CV, and repeated 10-fold CAP, all with 16 repetitions, supplementing Tables 1 and 2, respectively. They provide (i) comparisons between CV and

Table S1: Simulation results on overall | class 0 | class 1 risk prediction of the estimated classifier with three features

| n_0 $= n_1$ | rep. 2-fold CV | | rep. 10-fold CV | | rep. 10-fold CAP | | |
|------------------|----------------|------------|-----------------|----------|------------------|------------|------------------|
| | B | D | B | D | B | D | C |
| Scenario A | | | | | | | |
| 100 | 9 −10 15 | 20 59 32 | 3 −3 4 | 21 49 27 | 0 −2 | 1 21 40 24 | 94.2 94.1 94.8 |
| 200 | 4 −7 | 8 14 44 22 | 1 0 1 | 14 36 19 | 0 0 0 | 15 27 17 | 93.5 95.1 92.9 |
| 300 | 3 −8 | 7 11 38 18 | 0 0 0 | 11 31 15 | −1 −1 −1 | 12 23 13 | 94.4 94.6 95.2 |
| 400 | 2 −5 | 5 10 34 15 | 0 −2 1 | 10 27 13 | −1 −1 | 0 10 20 11 | 93.8 93.5 94.7 |
| 500 | 2 −2 | 3 9 30 13 | 0 1 0 | 9 24 11 | 0 0 0 | 9 18 10 | 93.7 95.5 93.7 |
| Scenario B | | | | | | | |
| 100 | 10 −12 17 | 21 56 32 | 4 −1 5 | 21 48 26 | 1 0 | 1 22 40 24 | 92.0 95.0 93.3 |
| 200 | 5 −7 | 9 14 40 21 | 1 1 1 | 14 35 18 | 0 1 −1 | 15 29 17 | 92.6 95.4 92.3 |
| 300 | 4 −11 | 9 11 35 18 | 0 −1 1 | 11 29 14 | 0 −1 | 0 11 23 12 | 94.1 94.7 94.2 |
| 400 | 3 −8 | 6 9 31 14 | 0 −3 1 | 9 25 12 | 0 −2 | 0 10 19 10 | 93.8 94.5 95.6 |
| 500 | 2 −6 | 5 8 29 13 | 0 −1 1 | 9 24 11 | 0 −1 | 0 9 19 | 9 93.0 94.1 94.7 |
| Scenario C | | | | | | | |
| 100 | 7 −9 13 | 20 60 33 | 0 −2 1 | 21 51 28 | −2 −4 −1 | 22 41 25 | 93.2 93.9 93.9 |
| 200 | 4 −9 | 9 15 46 23 | −1 −2 0 | 15 38 19 | −2 −2 −2 | 15 29 16 | 92.9 93.1 92.9 |
| 300 | 4 −14 11 | 12 39 20 | 0 −2 1 | 12 32 15 | −1 0 −1 | 12 24 13 | 94.0 94.9 95.2 |
| 400 | 4 −12 | 9 10 36 18 | 1 −1 1 | 10 28 14 | 0 1 | 0 10 20 11 | 94.8 94.9 94.6 |
| 500 | 3 −15 | 9 9 36 18 | 0 −3 1 | 9 27 13 | −1 0 −1 | 9 18 10 | 93.7 94.4 92.9 |
| Scenario D | | | | | | | |
| 100 | 9 −9 15 | 23 62 36 | 2 0 2 | 24 49 31 | −1 1 −2 | 24 39 28 | 93.1 95.5 92.7 |
| 200 | 5 −9 10 | 15 46 25 | 1 −2 2 | 15 35 20 | −1 0 −1 | 15 27 17 | 93.4 94.8 94.4 |
| 300 | 4 −9 | 8 12 39 19 | 0 0 0 | 12 31 16 | 0 −1 | 0 12 23 14 | 93.8 94.7 93.9 |
| 400 | 3 −7 | 6 9 34 16 | 0 −1 0 | 10 27 13 | −1 0 −1 | 10 20 11 | 93.7 94.6 94.1 |
| 500 | 2 −7 | 5 9 33 15 | 0 −2 0 | 9 26 12 | −1 0 −1 | 9 18 10 | 94.0 95.0 94.4 |

B: bias ($\times 1000$), D: mean absolute deviation ($\times 1000$), C: coverage probability of 95% risk bound (%).

CAP with the same fold number K and the same number of repetitions: repeated 2-fold CV versus repeated 2-fold CAP, and repeated 10-fold CV versus repeated 10-fold CAP; and (ii) a comparison between repeated 2-fold CAP and repeated 10-fold CAP. K -fold CV was sensitive to the choice of K , exhibiting larger positive bias for smaller values of K . In contrast, K -fold CAP showed little performance difference for different choices of K . These results further confirm that CAP outperforms CV, particularly for class-specific risks.

Table S2: Simulation results on overall | class 0 | class 1 risk prediction of the estimated classifier with six features

| n_0 $= n_1$ | rep. 2-fold CV | | | rep. 10-fold CV | | | rep. 10-fold CAP | | |
|------------------|----------------|----------|---------|-----------------|----------|----------|------------------|----------------|---|
| | B | D | | B | D | | B | D | C |
| Scenario A | | | | | | | | | |
| 100 | 13 −14 22 | 23 58 36 | 2 0 | 2 | 22 50 28 | −2 0 −2 | 24 42 28 | 91.2 93.4 91.5 | |
| 200 | 7 −9 12 | 15 43 23 | 0 −2 | 1 | 15 36 18 | −2 −1 −2 | 15 29 17 | 92.5 93.1 94.0 | |
| 300 | 5 −12 10 | 12 36 20 | 0 −2 | 1 | 12 29 16 | −1 0 −2 | 13 24 14 | 92.7 94.1 93.3 | |
| 400 | 4 −6 7 | 10 33 17 | 0 0 | 0 | 10 27 14 | −1 −1 −1 | 11 20 12 | 92.5 93.9 92.9 | |
| 500 | 5 −2 7 | 9 31 14 | 1 2 | 1 | 9 25 12 | 1 2 1 | 9 17 10 | 94.9 95.5 95.8 | |
| Scenario B | | | | | | | | | |
| 100 | 14 −17 25 | 24 53 38 | 2 −1 | 3 | 22 48 28 | −3 0 −3 | 25 42 28 | 88.4 94.1 88.5 | |
| 200 | 7 −11 13 | 15 42 23 | 0 −3 | 1 | 14 36 18 | −2 −1 −2 | 15 29 17 | 91.1 93.6 93.7 | |
| 300 | 5 −11 11 | 12 35 19 | 0 1 −1 | 11 | 30 15 | −1 1 −2 | 11 24 13 | 92.7 94.3 92.8 | |
| 400 | 5 −9 9 | 10 31 16 | 0 −2 | 1 | 10 26 13 | −1 0 −1 | 10 20 11 | 93.9 95.4 93.1 | |
| 500 | 5 −5 8 | 9 28 14 | 1 1 | 1 | 9 23 11 | 0 1 0 | 9 17 10 | 93.6 95.6 94.9 | |
| Scenario C | | | | | | | | | |
| 100 | 12 −15 21 | 24 58 39 | 1 −2 | 1 | 22 49 29 | −4 −3 −4 | 24 40 28 | 91.6 94.8 91.2 | |
| 200 | 8 −14 15 | 16 44 27 | 0 −2 | 1 | 16 37 20 | −2 0 −2 | 16 29 18 | 92.5 94.2 92.7 | |
| 300 | 7 −17 15 | 13 39 23 | 1 −2 | 1 | 12 31 16 | −1 0 −1 | 12 24 14 | 93.3 93.6 93.7 | |
| 400 | 5 −11 11 | 10 34 18 | 1 −1 | 2 | 10 27 14 | 0 1 −1 | 10 21 11 | 94.3 94.7 94.9 | |
| 500 | 5 −13 10 | 9 33 17 | 1 −3 | 2 | 9 26 13 | −1 0 −1 | 9 18 10 | 94.9 94.8 93.8 | |
| Scenario D | | | | | | | | | |
| 100 | 15 −15 25 | 25 59 40 | 3 0 | 4 | 22 50 30 | −1 2 −2 | 24 40 29 | 91.3 95.2 91.2 | |
| 200 | 8 −9 14 | 16 42 25 | 1 1 | 2 | 15 35 20 | 0 3 −1 | 16 28 18 | 93.1 95.8 92.9 | |
| 300 | 5 −15 12 | 12 41 22 | 0 −2 | 1 | 12 31 17 | −1 0 −1 | 12 22 14 | 92.7 94.2 95.3 | |
| 400 | 5 −9 9 | 10 35 18 | 0 −2 | 1 | 11 28 14 | −1 0 −1 | 11 21 12 | 92.8 94.3 93.5 | |
| 500 | 5 −6 8 | 9 32 16 | 1 0 | 1 | 9 25 13 | 0 0 0 | 10 18 11 | 94.6 93.5 95.2 | |

B: bias ($\times 1000$), D: mean absolute deviation ($\times 1000$), C: coverage probability of 95% risk bound (%).

D SIMULATION RESULTS OF LR-ERM CLASSIFICATION

LR-ERM classification is commonly used in practice when multiple features are present. It first employs logistic regression to combine features, followed by ERM to estimate the classification threshold. As noted in Remark 4, the resulting combination can be treated asymptotically as a fixed single feature for the purpose of model risk prediction. Under

the same set-ups in Section 4.1, Tables S3 and S4 present simulation results for model risk prediction with LR-ERM classification. The bootstrap method is that of Harrell, Lee, and Mark (1996) with 100 resamples, and repeat 2-fold CAP has 16 repetitions. The observed patterns were similar to those reported in Tables 1 and 2 with ERM classification.

Table S3: Simulation results on overall | class 0 | class 1 risk prediction of the LR-ERM classifier with three features

| n_0 | empirical | | | bootstrap | | | 10-fold CV | | | repeated 2-fold CAP | | |
|------------|-------------|----------|----------|-----------|----------|----------|------------|----------|----------------|---------------------|---|---|
| | B | D | C | B | D | C | B | D | C | B | D | C |
| Scenario A | | | | | | | | | | | | |
| 100 | -27 -26 -26 | 29 44 29 | -8 -8 -8 | 19 39 21 | -1 -2 -1 | 21 55 28 | -3 -3 -2 | 19 39 22 | 93.8 94.4 93.7 | | | |
| 200 | -16 -14 -16 | 18 30 19 | -4 -3 -4 | 13 28 15 | 1 -1 1 | 14 41 20 | 0 1 -1 | 13 28 15 | 95.2 95.1 95.5 | | | |
| 300 | -12 -11 -12 | 14 24 15 | -3 -2 -3 | 10 22 12 | 0 0 0 | 11 34 15 | 0 1 -1 | 10 22 12 | 95.4 95.8 95.0 | | | |
| 400 | -10 -10 -10 | 12 21 12 | -2 -2 -2 | 9 20 10 | 0 -2 1 | 10 32 14 | 0 0 0 | 9 20 10 | 94.8 95.4 95.1 | | | |
| 500 | -9 -8 -9 | 11 19 11 | -2 -2 -3 | 8 18 9 | 0 0 0 | 9 28 12 | -1 0 -1 | 8 18 9 | 94.5 94.5 95.2 | | | |
| Scenario B | | | | | | | | | | | | |
| 100 | -27 -24 -26 | 28 43 29 | -8 -6 -8 | 19 39 21 | -1 0 -1 | 21 53 27 | -3 -1 -3 | 19 39 22 | 93.5 94.6 94.1 | | | |
| 200 | -16 -14 -16 | 17 30 18 | -4 -3 -4 | 12 28 14 | 0 2 0 | 14 42 19 | 0 1 -1 | 13 28 15 | 94.5 95.4 94.4 | | | |
| 300 | -12 -12 -12 | 14 23 14 | -3 -3 -3 | 10 22 11 | 0 0 0 | 11 34 16 | -1 0 -1 | 10 22 12 | 95.5 95.0 95.9 | | | |
| 400 | -10 -10 -10 | 12 21 12 | -2 -3 -2 | 9 20 10 | 0 0 0 | 10 33 14 | 0 -1 0 | 9 20 10 | 94.8 94.1 95.2 | | | |
| 500 | -9 -9 -9 | 11 19 11 | -2 -3 -2 | 8 18 9 | 0 1 -1 | 9 28 13 | -1 -1 -1 | 8 18 9 | 93.7 94.2 94.5 | | | |
| Scenario C | | | | | | | | | | | | |
| 100 | -28 -28 -27 | 30 44 30 | -8 -7 -8 | 20 39 23 | 0 -3 1 | 23 60 32 | -2 -2 -2 | 21 39 24 | 93.4 94.5 93.3 | | | |
| 200 | -18 -17 -17 | 19 32 20 | -4 -4 -5 | 14 29 16 | 0 2 0 | 16 47 22 | 0 0 0 | 14 29 16 | 95.7 93.7 95.8 | | | |
| 300 | -14 -16 -13 | 16 26 17 | -4 -6 -3 | 12 23 14 | -1 0 -1 | 13 40 18 | -1 -3 -1 | 12 22 14 | 94.2 93.8 95.6 | | | |
| 400 | -11 -12 -10 | 13 21 13 | -2 -3 -2 | 10 19 11 | 0 1 0 | 11 34 16 | 0 -1 0 | 10 19 12 | 95.3 96.1 95.6 | | | |
| 500 | -9 -10 -9 | 11 19 12 | -2 -2 -2 | 9 18 10 | 0 1 0 | 10 31 14 | 0 0 0 | 9 18 10 | 95.0 94.8 95.8 | | | |
| Scenario D | | | | | | | | | | | | |
| 100 | -28 -23 -29 | 30 41 31 | -7 -5 -8 | 20 37 23 | 0 0 0 | 22 54 30 | -2 1 -2 | 20 37 23 | 95.2 95.2 94.0 | | | |
| 200 | -18 -15 -18 | 19 30 21 | -5 -4 -5 | 14 28 16 | -1 1 -1 | 15 44 21 | -1 -1 -1 | 14 28 16 | 95.0 94.0 94.9 | | | |
| 300 | -13 -12 -12 | 15 25 15 | -3 -4 -3 | 11 23 12 | 1 -2 1 | 12 38 17 | 0 -1 0 | 11 23 12 | 96.0 95.2 96.1 | | | |
| 400 | -11 -10 -11 | 13 22 13 | -3 -3 -2 | 10 20 11 | 0 0 0 | 11 33 15 | 0 -1 0 | 10 20 11 | 96.1 94.0 96.6 | | | |
| 500 | -9 -10 -9 | 11 19 12 | -2 -3 -2 | 9 18 10 | 0 0 0 | 9 31 14 | 0 -1 0 | 9 18 10 | 94.7 93.3 95.4 | | | |

B: bias ($\times 1000$), D: mean absolute deviation ($\times 1000$), C: coverage probability of 95% risk bound (%).

Table S4: Simulation results on overall | class 0 | class 1 risk prediction of the LR-ERM classifier with six features

| n_0 | empirical | | | bootstrap | | | 10-fold CV | | | repeated 2-fold CAP | | |
|-------|-------------|----------|----------|-----------|---------|----------|------------|----------|----------------|---------------------|----------|----------------|
| | B | D | C | B | D | C | B | D | C | B | D | C |
| n_1 | | | | | | | | | | | | |
| | Scenario A | | | | | | | | | | | |
| 100 | -32 -29 -31 | 32 45 32 | -6 -5 -7 | 19 38 21 | 2 1 2 | 22 57 30 | 1 2 1 | 20 39 23 | 94.8 96.0 93.7 | 1 2 1 | 20 39 23 | 94.8 96.0 93.7 |
| 200 | -19 -18 -19 | 20 31 21 | -4 -4 -4 | 13 28 15 | 0 0 0 | 14 42 20 | 0 0 0 | 13 28 15 | 95.0 95.0 94.3 | 0 0 0 | 13 28 15 | 95.0 95.0 94.3 |
| 300 | -14 -13 -14 | 16 25 16 | -3 -2 -3 | 11 23 12 | 0 1 0 | 12 38 17 | 0 1 0 | 11 23 12 | 95.7 95.7 94.8 | 0 1 0 | 11 23 12 | 95.7 95.7 94.8 |
| 400 | -11 -12 -11 | 13 22 13 | -2 -3 -2 | 9 20 10 | 1 0 1 | 10 34 15 | 0 0 1 | 9 20 11 | 96.8 95.3 95.9 | 0 0 1 | 9 20 11 | 96.8 95.3 95.9 |
| 500 | -10 -10 -9 | 11 20 11 | -2 -3 -1 | 8 19 9 | 1 0 1 | 9 30 13 | 1 -1 1 | 8 18 9 | 94.9 94.3 95.8 | 1 -1 1 | 8 18 9 | 94.9 94.3 95.8 |
| | Scenario B | | | | | | | | | | | |
| 100 | -31 -28 -30 | 32 44 32 | -5 -3 -6 | 18 38 20 | 3 0 4 | 20 57 28 | 1 3 1 | 19 38 22 | 94.9 95.4 94.8 | 1 3 1 | 19 38 22 | 94.9 95.4 94.8 |
| 200 | -19 -18 -19 | 21 31 21 | -4 -4 -5 | 13 28 15 | 0 -1 0 | 14 42 20 | 0 0 0 | 13 28 15 | 95.7 95.1 94.6 | 0 0 0 | 13 28 15 | 95.7 95.1 94.6 |
| 300 | -15 -14 -14 | 16 25 16 | -3 -3 -3 | 10 23 12 | 0 -1 0 | 11 37 16 | 0 0 -1 | 10 23 12 | 95.7 94.0 94.9 | 0 0 -1 | 10 23 12 | 95.7 94.0 94.9 |
| 400 | -11 -11 -11 | 13 22 13 | -2 -2 -2 | 9 20 10 | 1 0 1 | 10 33 15 | 0 1 0 | 9 20 10 | 95.4 94.2 94.9 | 0 1 0 | 9 20 10 | 95.4 94.2 94.9 |
| 500 | -10 -11 -9 | 11 20 11 | -2 -3 -1 | 8 18 9 | 1 -3 2 | 9 30 13 | 0 -1 1 | 8 18 9 | 95.9 94.0 95.8 | 0 -1 1 | 8 18 9 | 95.9 94.0 95.8 |
| | Scenario C | | | | | | | | | | | |
| 100 | -35 -36 -33 | 35 47 35 | -8 -8 -8 | 21 38 23 | 1 -5 2 | 23 61 33 | 0 -1 0 | 21 38 25 | 95.3 95.1 95.0 | 0 -1 0 | 21 38 25 | 95.3 95.1 95.0 |
| 200 | -22 -21 -21 | 22 32 23 | -5 -4 -5 | 14 29 17 | -1 -1 0 | 15 47 23 | -1 0 -1 | 14 28 16 | 95.0 94.5 95.7 | -1 0 -1 | 14 28 16 | 95.0 94.5 95.7 |
| 300 | -15 -13 -15 | 16 24 17 | -2 -1 -3 | 11 22 13 | 2 0 2 | 13 43 20 | 1 3 0 | 11 22 13 | 95.9 95.6 95.1 | 1 3 0 | 11 22 13 | 95.9 95.6 95.1 |
| 400 | -13 -13 -13 | 15 22 15 | -3 -3 -3 | 10 20 12 | 0 0 0 | 11 38 17 | 0 0 0 | 10 20 12 | 95.2 94.6 95.1 | 0 0 0 | 10 20 12 | 95.2 94.6 95.1 |
| 500 | -11 -11 -11 | 12 19 13 | -2 -2 -2 | 9 18 10 | 1 1 1 | 10 34 14 | 0 0 0 | 9 18 10 | 94.7 95.3 95.1 | 0 0 0 | 9 18 10 | 94.7 95.3 95.1 |
| | Scenario D | | | | | | | | | | | |
| 100 | -35 -32 -35 | 36 45 37 | -8 -8 -9 | 21 38 23 | 0 -4 1 | 22 57 31 | -1 -1 0 | 21 37 25 | 94.0 95.3 93.7 | -1 -1 0 | 21 37 25 | 94.0 95.3 93.7 |
| 200 | -20 -18 -20 | 21 31 22 | -4 -3 -4 | 13 28 15 | 1 -2 2 | 15 46 20 | 1 1 1 | 13 29 15 | 95.8 94.8 95.7 | 1 1 1 | 13 29 15 | 95.8 94.8 95.7 |
| 300 | -15 -14 -15 | 16 26 17 | -3 -2 -3 | 11 23 13 | 1 3 0 | 13 40 18 | 1 1 1 | 11 23 13 | 97.0 94.5 96.6 | 1 1 1 | 11 23 13 | 97.0 94.5 96.6 |
| 400 | -13 -11 -13 | 14 22 15 | -3 -2 -3 | 9 21 11 | 0 -1 0 | 10 36 16 | 0 0 0 | 9 21 11 | 96.0 94.8 95.9 | 0 0 0 | 9 21 11 | 96.0 94.8 95.9 |
| 500 | -10 -10 -10 | 12 20 12 | -2 -2 -2 | 9 18 10 | 0 -2 1 | 10 31 14 | 1 0 1 | 9 18 10 | 95.9 94.4 96.1 | 1 0 1 | 9 18 10 | 95.9 94.4 96.1 |

B: bias ($\times 1000$), D: mean absolute deviation ($\times 1000$), C: coverage probability of 95% risk bound (%).